



**QUEEN'S
UNIVERSITY
BELFAST**

Circular economy approach of enhanced bifunctional catalytic system of CaO/CeO₂ for biodiesel production from waste loquat seed oil with life cycle assessment study

Al-Muhtaseb, A. H., Osman, A. I., Kumar, P. S. M., Jamil, F., Al-Haj, L., Al Nabhani, A., Kyaw, H. H., Myint, M. T. Z., Mehta, N., & Rooney, D. W. (2021). Circular economy approach of enhanced bifunctional catalytic system of CaO/CeO₂ for biodiesel production from waste loquat seed oil with life cycle assessment study. *Energy Conversion and Management*, 236, Article 114040.

Published in:
Energy Conversion and Management

Document Version:
Peer reviewed version

Queen's University Belfast - Research Portal:
[Link to publication record in Queen's University Belfast Research Portal](#)

Publisher rights

Copyright 2021 Elsevier.

This manuscript is distributed under a Creative Commons Attribution-NonCommercial-NoDerivs License

(<https://creativecommons.org/licenses/by-nc-nd/4.0/>), which permits distribution and reproduction for non-commercial purposes, provided the author and source are cited.

General rights

Copyright for the publications made accessible via the Queen's University Belfast Research Portal is retained by the author(s) and / or other copyright owners and it is a condition of accessing these publications that users recognise and abide by the legal requirements associated with these rights.

Take down policy

The Research Portal is Queen's institutional repository that provides access to Queen's research output. Every effort has been made to ensure that content in the Research Portal does not infringe any person's rights, or applicable UK laws. If you discover content in the Research Portal that you believe breaches copyright or violates any law, please contact openaccess@qub.ac.uk.

Open Access

This research has been made openly available by Queen's academics and its Open Research team. We would love to hear how access to this research benefits you. – Share your feedback with us: <http://go.qub.ac.uk/oa-feedback>

Circular Economy Approach of Enhanced Bifunctional Catalytic System of CaO/CeO₂ for Biodiesel Production from Waste Loquat Seed Oil with Life Cycle Assessment Study

Ala'a H. Al-Muhtaseb^{1*}, Ahmed I. Osman^{2,3*}, Paskalis Sahaya Murphin Kumar^{1,4*}, Farrukh Jamil⁵, Lamyia Al-Haj^{6*}, Abdulrahman Al Nabhani⁷, Htet Htet Kyaw⁸, Myo Tay Zar Myint⁹, Neha Mehta¹⁰, David W. Rooney²

¹Department of Petroleum and Chemical Engineering, College of Engineering, Sultan Qaboos University, Muscat-Oman

²School of Chemistry and Chemical Engineering, Queen's University Belfast, Belfast-Northern Ireland, UK

³Nanocomposite Catalysts Lab., Chemistry Department, Faculty of Science at Qena, South Valley University, Qena 83523, Egypt.

⁴Department of Civil and Environmental Engineering, Yonsei University, Seoul 03722, Republic of Korea

⁵Department of Chemical Engineering, COMSATS University Islamabad, Lahore-Pakistan

⁶Department of Biology, College of Science, Sultan Qaboos University, Muscat-Oman

⁷Electron Microscopy Unit, College of Medicine & Health Sciences, Sultan Qaboos University, Muscat-Oman

⁸Nanotechnology Research Center, Sultan Qaboos University, Muscat-Oman

⁹Department of Physics, College of Science, Sultan Qaboos University, Muscat-Oman

¹⁰School of Mechanical and Aerospace Engineering, Queen's University Belfast, Belfast, Northern Ireland, UK

*Those authors contributed equally

***Corresponding authors:**

Dr Ala'a H. Al-Muhtaseb (muhtaseb@squ.edu.om)

Dr Ahmed I. Osman (aosmanahmed01@qub.ac.uk)

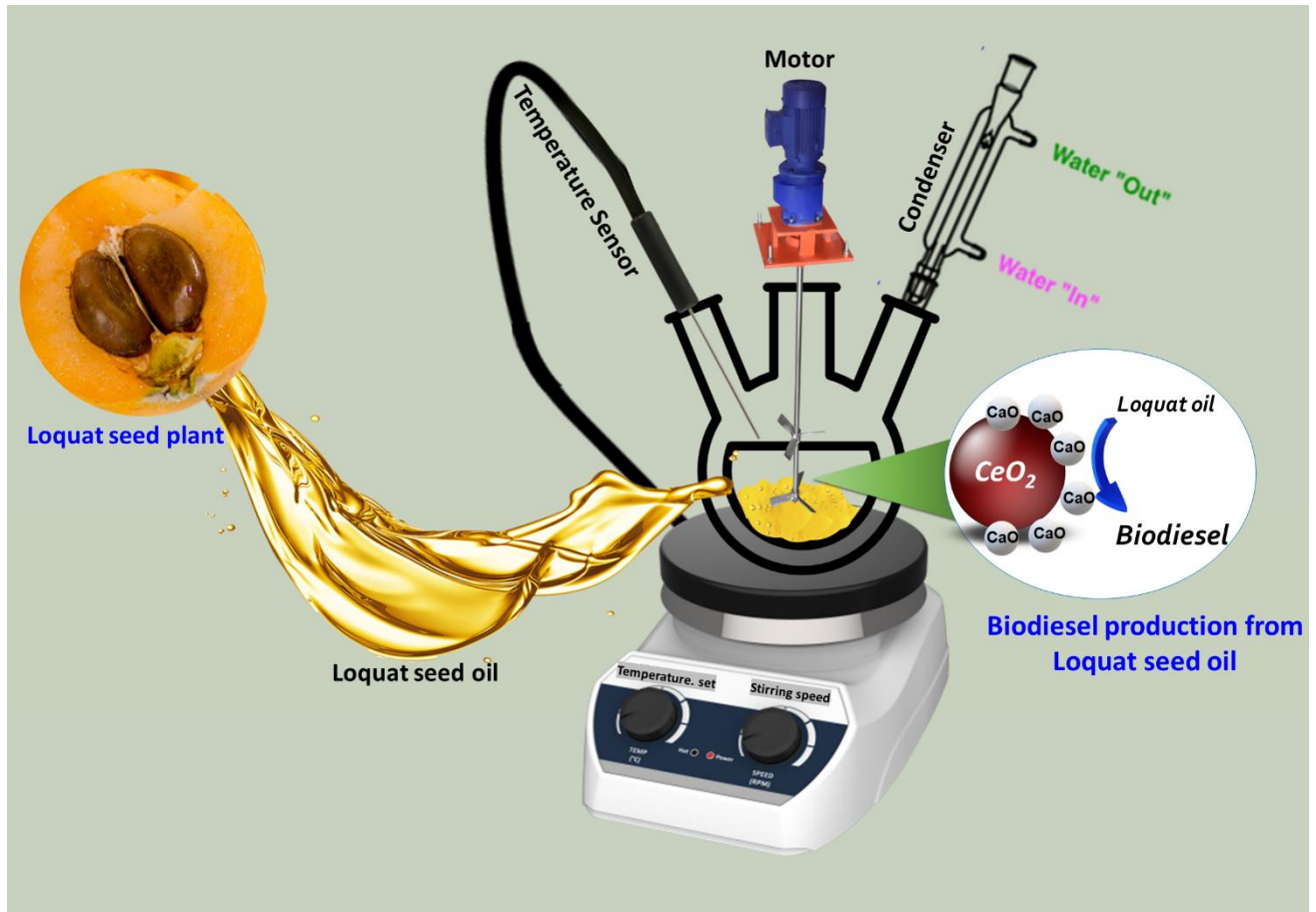
Dr Lamyia Al-Haj (lamya@squ.edu.om)

Abstract:

Herein, we utilised Loquat seed oil as a waste resource to produce biodiesel over a novel bifunctional catalyst system based on CaO loaded on a ceria oxide support. The catalysts were characterised using XRD, SEM-EDX, SBET STEM, and TPD analyses, followed by parametric analysis to optimise the catalyst performance. The XPS analysis showed a strong synergistic effect between CaO and CeO₂ support. The parametric study revealed that the most active catalyst (15 wt.% CaO-CeO₂) showed optimum biodiesel yield was 90.14 (\pm 0.1) wt.% at a temperature of 70 °C, methanol: oil of 9, time of 90 minutes and 4 wt.% of catalyst. The reusability test showed that when the most active catalyst was calcined and reused, the biodiesel yield was almost the same \pm 0.5%; however, when biodiesel production was used without calcination, the biodiesel yield was reduced by 15%. The quality of the produced biodiesel was investigated by the American Society for Testing and Materials (ASTM) and European Union (EU) Standards. It showed that it satisfied all standards and could be used as potential alternative fuel instead of fossil diesel from novel Loquat seed oil. The Life Cycle Assessment (LCA) results using midpoint indicators (from CML-IA baseline V3.06 method) showed the cumulative abiotic depletion of fossil resources over the entire process of biodiesel production was 26349 MJ, global warming potential was 1129 kg CO₂ eq, and human health toxicity was 422 kg 1,4-DB eq (kg 1,4 dichlorobenzene equivalent). The highest damage in most environmental categories was observed during catalyst preparation and regeneration. This was confirmed in endpoint LCA findings (ReCiPe 2016 Endpoint (E) V1.04), where catalyst preparation contributed to human health (119.2 Pt), ecosystems damage (9.3 Pt) and resources depletion (0.5 Pt). Furthermore, the energy ratio was 2.23 for the biodiesel production process (computed as output energy/input energy) by considering allocation of output energy due to biodiesel and glycerol.

Keywords: Biodiesel, Bifunctional catalyst, Waste loquat seed, Circular economy, Life cycle assessment.

Graphical abstract



1. Introduction

Nowadays, the use of petroleum-based fuels is still dominating the transport sector worldwide. It is estimated that with time, reservoirs of petroleum fractions will become empty and eventually will deplete [1]. Another problem with these petroleum products is that they emit toxic gases in the atmosphere when combusted. These toxic gases are greenhouse gases that are known to cause global warming, climate change and environmental pollution [2-5]. These toxic greenhouse gases are also known to have adverse human health impacts with their carcinogenic effect [2, 3]. Considering the above reasons, it is necessary to find an alternative energy source that should be environmentally friendly and meets our energy demand [6, 7]. Biodiesel derived from agricultural waste can provide a potential alternative [8-13].

Initially, during World War 2, when petroleum supplies were interrupted, pure vegetable oil was used in diesel engines in many countries. However, when the war ended and petroleum fractions became cheap again, vegetable oil fuel was forgotten [14-16]. Modern-day biodiesel fuel is made by transesterification reactions, in which vegetable oil is converted into fatty acids methyl esters. Biodiesel can be produced from several feedstocks that include all oils derived from biomass, vegetable oil, or animal fats [17, 18]. As biodiesel is obtained by processing biomass-derived oils; thus, it is seen as environmentally friendly and biodegradable[19].

Conventional diesel engines have been tested using biodiesel when blended with fossil diesel in different fractions as well as for pure biodiesel, and it was concluded that no modification is required in the engine [20, 21]. Moreover, vegetable oil has a higher viscosity and low calorific value; thus, transesterification reduces molecular weight to one third, and a reduction in viscosity is achieved, essentially making the oil more suitable as an engine fuel [22, 23].

The transformation of biomass-derived oil to biodiesel is carried out via catalytic transesterification, which involves the reaction between triglyceride and alcohol in the presence of a suitable catalyst that results in methyl formation ester and glycerol [24, 25]. As triglyceride consists of a glycerin molecule as a backbone element of which three long-chain fatty acids are linked, the characteristic properties of oil vary depending on the nature of the attached fatty acids with a basic glycerin molecule. It has been reported that variation in oil composition, which depends on feedstock properties, can result in biodiesel characteristics. Initially, biodiesel production is performed in the presence of a homogeneous catalyst which includes alkali hydroxides such as sodium (NaOH), potassium (KOH) hydroxides, and sodium methoxide as a catalyst [26].

Oil composition and properties are important factors for deciding the protocol to be followed for oil transformation into biodiesel [27]. Oil with a higher free fatty acid content needs to be pre-treated prior to transesterification. The pre-treatment of oil with high fatty acid content is done by esterification, which involves the free fatty acids reaction with alcohol in the presence of an acid catalyst that results in water formation and methyl esters. Most commonly, esterification is done with the aid of sulfuric acid as an acid catalyst. In the commercialisation of biodiesel, its high cost is a major barrier. The main factor is its feedstock which normally accounts for 70-80 % of the biodiesel production cost. Nonedible feedstocks are the most appropriate solution for this issue [28, 29]. Plenty of nonedible feedstocks have been reported for biodiesel production, such as jatropha seed oil, rubber seed oil, palm kernel shell oil and date seed oil. Loquat fruit is grown and has been used for more than 1000 years [30]. It contains 2-3 seeds which occupy almost 10-20 wt. % of the total fruit, and these seeds can be used as a novel source of bio-oil, which can be further used in biodiesel production [31].

Despite this, nonedible oil encounters a major issue via its transformation into biodiesel due to the presence of high content of free fatty acids. Thus, a two-step process is recommended; this involves esterification followed by transesterification to produce biodiesel [29, 32-34]. To avoid the two-step process, a study has reported the efficient synthesis and usage of a bifunctional catalyst that possesses active acidic and basic sites to promote esterification and transesterification. Hassan et al. reported a bi-functional catalyst for nonedible oil, and a high biodiesel yield (>90%) was obtained [35]. Farooq et al. synthesised a highly efficient bifunctional catalyst and applied it to waste cooking oil with high FFA content, and obtained a high conversion and biodiesel yield (>90%) [36]. Similarly, it was reported the efficient usage of Mn@MgO-ZrO₂ as a bi-functional catalyst obtained a high biodiesel yield (>90%) when waste date seeds oil was used as a feedstock [37]. Thus, based on the need for an efficient bifunctional catalyst, this study intended to report the synthesis of an efficient catalyst to be used on a nonedible oil.

Moreover, there is a lack of environmental impact study for biodiesel production from loquat seed oil. If loquat seed oil is to be widely recognised in the biodiesel field, environmental impact studies are necessary to measure the potential impacts of the production process. The life cycle assessment (LCA) research has been conducted for various bioenergy systems, including biofuels. LCA is a systematic tool that evaluates the environmental impacts of a product through the entire production process, including the primary production process and final disposal after use (ISO, 2006) [38].

Therefore, the current study aimed to use loquat seeds as a novel oil source for biodiesel production and evaluate environmental impacts using LCA for the entire process. For biodiesel production, a bi-functional catalytic system was synthesised based on the promotion of CaO on CeO₂ support and further characterised using various techniques to investigate their feasibility in the biodiesel production process. The produced biodiesel quality was investigated and benchmarked using the

American Society for Testing and Materials (ASTM) and European Union (EU) Standards. Biodiesel obtained as the end product was evaluated by determining its fuel properties and evaluating the environmental impacts of the entire process using LCA. The current work shows the potential of nonedible (loquat seeds) agricultural waste for biodiesel production and synthesis of a novel heterogeneous catalyst; thus, both these factors will lead to the economical production of biodiesel.

2. Materials and methods:

2.1 Materials

Loquat seeds oil was extracted using a soxhlet extractor. Chemicals were purchased from Sigma-Aldrich; calcium nitrate tetrahydrate ($\text{Ca}(\text{NO}_3)_2 \cdot 4 \text{H}_2\text{O}$) (99.9%), cerium nitrate hexahydrate ($\text{Ce}(\text{NO}_3)_3 \cdot 6\text{H}_2\text{O}$) (99.8%), ethanol and plant powder.

2.2 Synthesis of catalyst and characterisation

500 mg of cerium nitrate hexahydrate was dissolved in 50 mL of ethanolic plant extract and stirred for 4 hours to obtain a homogenous solution. The solution mixture was transferred into the Teflon lined autoclave (100 mL) and heated at 180 °C for 12 hours. After the reaction was terminated, the autoclave was allowed to cool down to room temperature. The obtained precipitate was centrifuged and washed at 3000 rpm for 20 min with deionised water and ethanol. The same procedure was followed to synthesise the composite with the addition of a calculated amount of calcium nitrate tetrahydrate to attain 5 to 20 % CaO supported CeO_2 . The X-ray diffraction (XRD) patterns were acquired by using the X'Pert PRO Analytical X-ray diffractometer. The X-ray photoelectron spectra (XPS) were obtained using a monochromatic Al $K\alpha$ X-ray source (Omicron Nanotechnology, Germany). The morphologies of the fabricated nanostructures were inspected using a field emission scanning electron microscope (FESEM: JEOL JSM 7800F, Japan) operated

at 15 kV accelerating voltage. In order to determine the physiochemical properties, Brunauer-Emmett-Teller (BET) model ASAP 2020, purchased from Micromeritics Instruments Inc., Norcross, GA, USA, was used. Temperature programmed desorption technique (TPD) (TPDRO 1100 Series Thermo Finnigan) consuming carbon dioxide and ammonia gasses for quantifying active sites of the prepared catalyst was used.

The thermogravimetric analysis was conducted using (TGA, Perkin Elmer Pyris STA 6000) at a heating rate of 10 °C/min from 30° to 900 °C under a nitrogen gas atmosphere. The nitrogen flow rate was 20mL/min. Fourier Transform Infrared spectroscopy (FTIR) spectra were recorded by infrared spectroscopy (PerkinElmer, SpectraOne, USA) with KBr pellets in the range 400–4000 cm^{-1} . The signal resolution of 4 cm^{-1} with 40 scans was applied.

2.3 Biodiesel production using the synthesised catalyst

To evaluate the applicability of prepared catalysts for Loquat seed oil reaction with alcohol, all experiments were conducted based on the parameters and their ranges [39] mentioned in Table 1. Two neck flasks are used as a reaction vessel attached to the condenser for continuous refluxing of methanol in the reaction vessel. Initially, oil was poured into the vessel and heated up to the desired temperature according to the desired reaction condition. Methanol was then mixed with a catalyst and poured into a reaction vessel containing the heated oil. The reaction was carried out for the required time, and then heating was stopped, and the reaction mixture was allowed to cool down, followed by pouring it into a separator funnel. After allowing the reaction mixture to stay for 4 hours in a separatory funnel, the product (biodiesel) and by-product (glycerol) were separated into two layers. The bottom layer of glycerol was removed, and the remaining biodiesel was washed thoroughly with warm water.

Table 1: The parameters used herein for the production of biodiesel from waste loquat seed oil.

<i>Parameters</i>	<i>Low limit</i>	<i>High limit</i>
<i>Temperature (°C)</i>	50	80
<i>Time (min)</i>	30	120
<i>Methanol to oil ratio</i>	6	15
<i>Catalyst (wt. %)</i>	2	8

Furthermore, biodiesel was collected in an airtight vessel and was characterised to determine the fuel properties. Biodiesel was analysed by GC-MS from Perkin Elmer using the DB-Wax column. For quality analysis, several techniques involving using standard methods were used, such as the D-2500 method for determining cold point, D-97 method for measuring pour point and measuring cold filter plugging point, D-6371 was utilised. D-664 for acid value, flash point of biodiesel was determined by D-93, D-613 method was used for determining cetane number, and the method adopted was D-445 for measuring kinematic viscosity. Each experimental result reported herein from the triplicate performance to ensure the reproducibility of the results.

3. Results and discussion

3.1 Catalyst characterisation

X-ray powder diffraction analysis was conducted to determine the crystal planes of the synthesised catalysts, as shown in Figure 1a. The characteristic diffraction lines of pristine CeO₂ are at 2θ = 28.6° (111), 33.1° (200), 47.6° (220), 56.5° (311), 59.2° (222), 69.4° (400), 76.7° (331), and 79.1° (420) (JCPDS (PDF) no. 43–1002) based on cubic fluorite structure of CeO₂ [40]. Thus, based on the XRD diffraction lines, it was obvious that the pristine catalyst was crystalline in nature, along with the modified catalysts as well. The diffraction lines of the CaO/CeO₂ nanomaterial gave rise to some new diffraction lines at 26.8° and 32.2°, which can be attributed to active material calcium

oxide (PDF no. 00-004-0777&00-017-0912, JCPDS). The addition of CaO at low concentrations on pristine CeO₂, i.e. 5% CaO/CeO₂, has not affected the phase of material and maintained the crystalline phase. While at high concentrations >10% CaO/CeO₂, the Ca metal diffraction lines started to appear at $2\theta = 24.7^\circ$ and 43.7° [41]. The FTIR spectra of the modified catalysts showed that at low Ca loadings, i.e., 5% CaO/CeO₂ catalyst, small absorption bands at 875 and 1468 cm⁻¹, which are attributed to the symmetric stretching vibration of carbonate (Figure 1b) [42]. Those carbonate bands were increased with increasing the % wt. Ca over the CeO₂ support. This is due to the interaction between the doped CaO and the carbon dioxide, which led to the carbonate formation. Furthermore, with the Ca loadings, the hydrophilicity of the modified catalysts has increased, as shown from the O-H stretching vibrations that appeared at absorption bands around 3400 cm⁻¹ (highlighted box in Figure 1b).

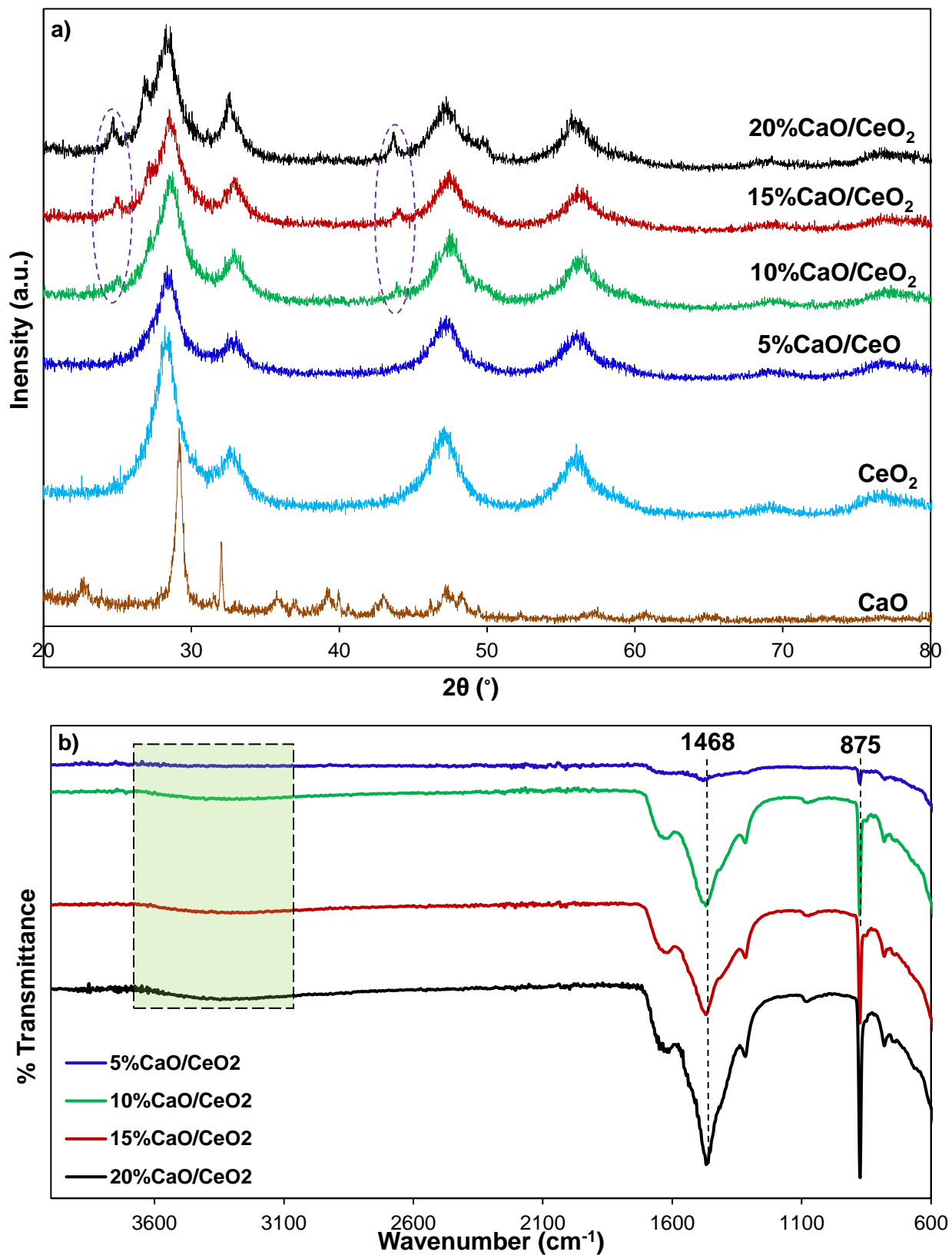


Figure 1: shows a) XRD patterns and b) FTIR spectra for CaO modified CeO₂ catalysts.

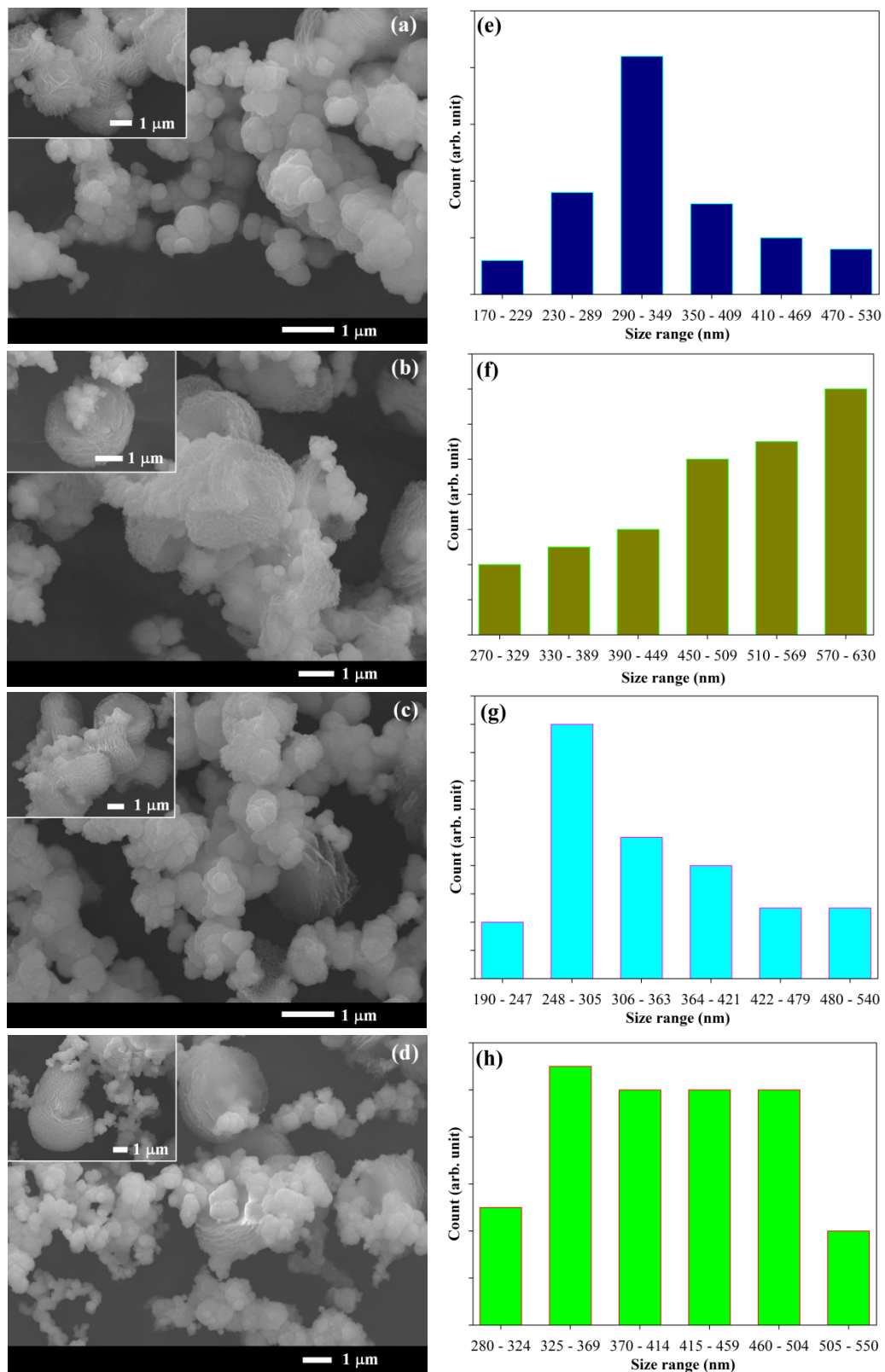


Figure 2: FESEM images for synthesised CaO/CeO₂ catalysts and size distribution histogram of (a - e) CaO 5 % (b - f) CaO 10 % (c - g) CaO 15 % (d - h) CaO 20 %.

The FESEM images in Figure 2 a-d show the surface morphology of CaO/CeO₂ catalysts with different loading of CaO (5, 10, 15 and 20 wt.%). Based on the SEM images, it can be observed that all catalyst samples were mainly composed of isotropic shaped particles and accumulated form. Two different types of particle shapes were noticed: isotropic with a rough surface (nano-scale) and flake type donut shape particle (micro-scale) (See Figure 2 a-d: Inset). Figure 2 e-f shows the particle size distribution of the fabricated catalyst samples (the particles were counted on the isotropic shaped particle), with the size ranging from 200 nm to 600 nm. The highest particle count of CaO 5 % was observed at the size range of 300-350 nm, CaO 10 % at 570-630 nm, but, small size range also dominated, CaO 15 % at 250-300 nm but a wide range of high particle count was observed ranging from 325 nm to 500 nm for CaO 20 %. This could be one of the reasons to decrease the catalytic performance in biodiesel conversion.

Interestingly, the second type of particle (so-called flake type donut shape) size increased while CaO content increased with an average size of 2.4 μm for CaO 5 % and CaO 10 % and 3.5 μm for CaO 15 % and 4.3 μm for CaO 20 % respectively. Moreover, calcium was well distributed on the support CeO₂, which was confirmed from the elemental mapping for each sample, as shown in Figure S1 (Supplementary Information). The uniform distribution of active material is crucial for material to be used as a catalyst for the chemical reaction. A rough surface makes high active areas, which could contribute to the transesterification process to produce biodiesel.

Figure 3a shows the XPS survey spectra of 5, 10, 15 and 20 % CaO/CeO₂ samples. Apart from the expected elements such as Ce, Ca, O and C on the sample surfaces, no other contaminations were detected. Figure 3b-d shows the core level XPS spectra of Ce 3d, O 1s and Ca 2p, respectively. Binding energy (BE) shift was observed to a lower value while increasing Ca content, and this shift was observed for the core level Ce, Ca and O. This substantial BE shift was observed while

CaO was increased from 5 to 10 wt.%, but no more shift was witnessed for the 15 and 20 wt.% sample (See Figure 3b-d). This may be due to the CaO content on the catalyst surface was saturated at these high concentrations.

Moreover, this lower BE shift has affirmed the chemical interaction between CaO-CeO₂. Yu *et al.* reported the correlation between BE shift with respect to basic strength where BE decreased, the basic strength increased [43]. In our case, the BE shifted to lower values, which were in good agreement with TPD results (see Figure 3c and Table 2). Figure 3b shows the deconvoluted Ce 3d peaks composed with characteristic peaks of the two oxidation states of Ce (Ce³⁺ and Ce⁴⁺), which were detected, and the satellites were also observed. Figure 3c shows the presence of Ca on the catalyst surface, and it was increased while increasing CaO content.

In contrast, Ca content on the catalyst surface decreased drastically for the 20 wt.% CaO/CeO₂ sample (see Figure 3e). This must be one of the reasons why biodiesel production yield of 20 wt.% CaO-CeO₂ catalyst was decreased (Figure 6). In general, the inclusion of CaO on parent CeO₂ enhanced the catalytic activity, thus improved biodiesel production yield.

Moreover, Figure 3e depicted the surface oxygen and Ce components decreased while Ca content increased. The surface concentration of Ce decreased notably for the 10 wt.% CaO-CeO₂ sample but was almost the same for the 15 and 20 wt.% CaO-CeO₂ samples. Thus, it can be concluded that due to the addition of CaO, change in the oxidation state and the chemical environment of material occurs, resulting in a more stable material, which can help avoid leaching when used for chemical reactions.

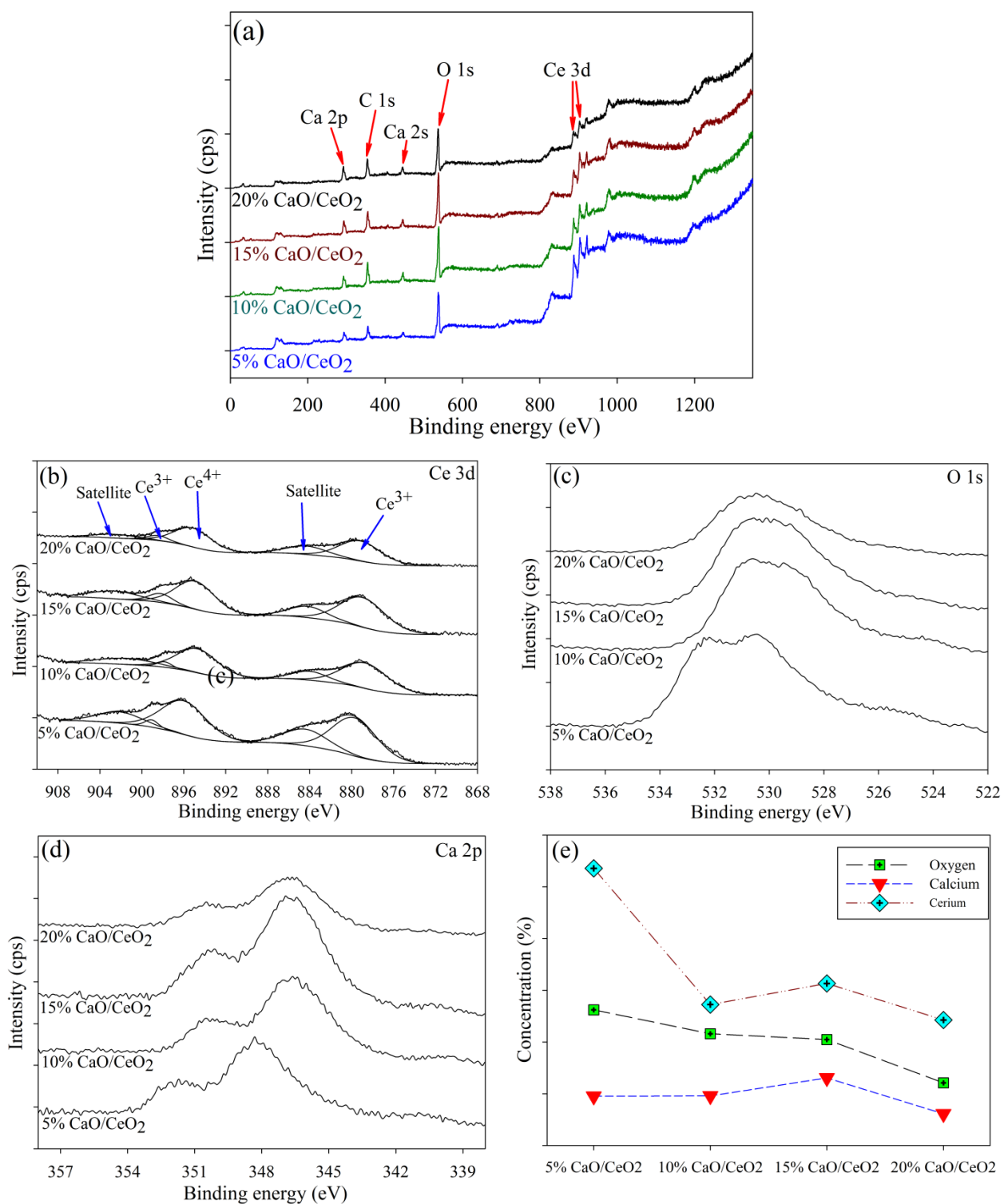


Figure 3: (a) XPS survey spectra of 5, 10, 15, and 20 % CaO/CeO₂ catalysts with XPS spectra (b) Ce 3d (c) O 1s (d) Ca 2p (e) Surface concentration (%) of O, Ca and Ce (The concentration was estimated from area under the graph of high-resolution XPS spectra of O 1s, Ca 2p and Ce 3d respectively)

Temperature programmed desorption TPD study was conducted to determine the acidic and basic active sites, as shown in Table 2, which shows the strength of the active site along with their % contribution over the synthesised catalysts. Support material CeO_2 possesses the lowest overall quantities of basic and acidic active sites, with values of 0.098 and 0.077 mmol/g, respectively, compared to 2-3 mmol/g for the modified catalysts. However, the modified catalyst active sites strength varied with different strengths, according to different CaO loadings. In general, the strong basic sites increased with increasing the CaO loadings, which might be due to the basic nature of the CaO resultant catalyst surface changed to valence basic nature material. It can be observed that overall basic sites continued to increase until the concentration of CaO on CeO_2 was increased to 15 wt%. Beyond that, it decreased, which can be related to the fact that excess CaO resulted in it filling and blocking the pores and due to which active sites are blocked and will not be exposed to reactants resulting the decreased basic strength (from 3.191 to 2.985 mmol/g). Further on, despite being basic in nature, CaO metallic oxide resulted in a small number of acidic sites to parent material CeO_2 , as shown in Table 2. Thus, it can be concluded that the resultant material becomes active as acidic and basic, showing high suitability for reaction leading to biodiesel production from nonedible oils.

Table 2: Temperature programmed desorption analysis for synthesised catalysts

<i>Catalyst</i>	<i>Basic *</i>	<i>Strength</i>		<i>Acidic*</i>	<i>Strength</i>	
		Weak (%)	Strong (%)		Weak (%)	Strong (%)
<i>CeO₂</i>	0.098	39.32	60.68	0.077	61.23	38.77
5 wt.% CaO-CeO ₂	2.182	54.28	45.72	0.134	52.62	47.38
10 wt.% CaO-CeO ₂	3.013	56.92	43.08	0.925	50.37	49.63
15 wt.% CaO-CeO ₂	3.191	53.27	46.73	1.021	51.23	48.77
20 wt.% CaO-CeO ₂	2.985	53.94	46.06	1.042	53.78	46.22

*(milli-moles per gram)

BET results revealed the physicochemical properties of synthesised catalysts which are shown in Table 3 and Figure 4a. The specific surface area of the parent material was not high; but, it started increasing with the addition of CaO, along with the pore volume, as shown in Figure 4a. The increment in the surface area resulted from the interaction between the metallic oxides (CeO₂-CaO), which tends to open new pores and increase the externally exposed surface of the material. Moreover, this can be related to results reported in the XPS analysis (Figure 3), which depicted the strong interaction between the metallic oxides. Further on, the increment in the surface area when the metallic oxide CaO was increased until 15 wt.% over CeO₂ and beyond that had started decreasing, which infers to elevated concentration may tend the metallic oxides to fill the pores and form clusters, then consequently decreasing the surface area of resultant material (CaO-CeO₂). It has been reported that the particle diameter of triglyceride is 5.8 nm [44]. Thus, the material used as a catalyst involving triglycerides as reactants should have high pore diameters to get the maximum product yield. Therefore, the synthesised catalysts are suitable for biodiesel production as it involves the triglycerides and methanol as reactants. The TGA curves of the modified catalysts

are shown in Figure 4b, where the % weight loss was increasing with increasing the % CaO loadings. This agrees with the previously published work of Anand et al., who reported a similar decomposition temperature at around 800 °C [45]. Clearly, there were three-stages of mass loss; 110-215, 215-615 and 615-820 °C, respectively which are attributed to the water desorption, carbonate decomposition and the CeO₂ support, and finally, CaO decomposition.

Table 3: BET analysis for determination of physicochemical characteristics

<i>Catalyst</i>	<i>Specific surface area</i>	<i>Pore volume (cm³/g)</i>	<i>Average pore size</i>
CeO ₂	15.23	0.09	5.65
5 wt.% CaO-CeO ₂	33.59	0.22	7.32
10 wt.% CaO-CeO ₂	38.13	0.39	8.01
15 wt.% CaO-CeO ₂	39.65	0.51	7.87
20 wt.% CaO-CeO ₂	35.26	0.47	8.19

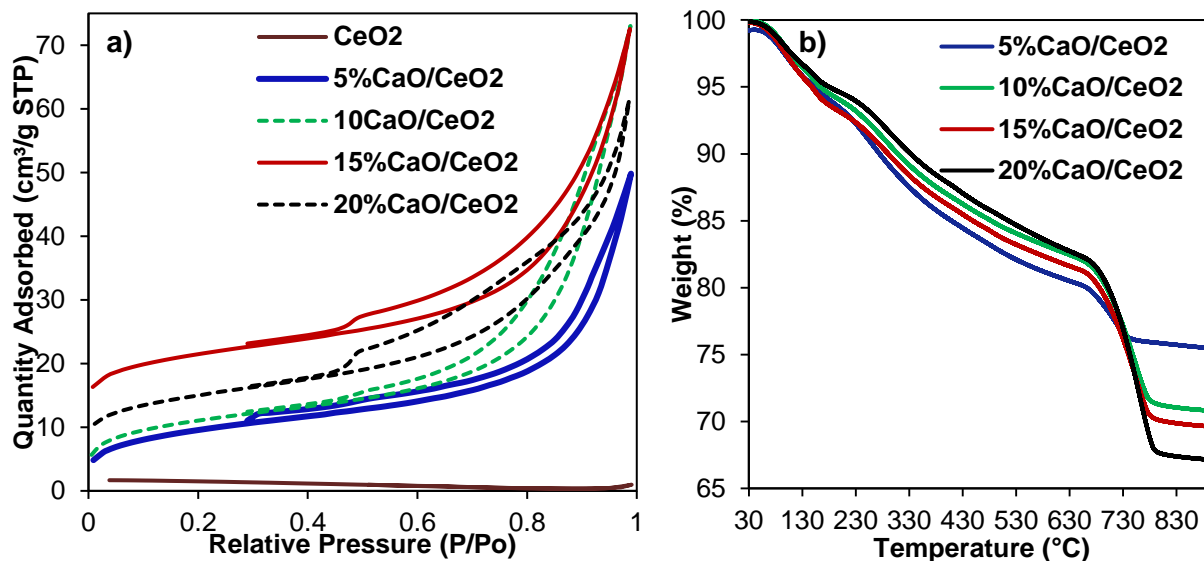


Figure 4: shows a) adsorption-desorption isotherms and b) TGA curves for CaO modified CeO₂ catalysts.

Figure 5 a-e shows the elemental mapping of the pristine CeO_2 support, along with CaO modified catalysts. From the mapping, Ce, O and Ca were detected without any impurities. The bright-field (BF) images (Figure 5 a-e) show the particle shape of the pristine CeO_2 , as well as CaO modified catalysts, which were isotropic shape, as shown in Figure 5. It is not surprising that the elemental mapping of the presence of Ca was increasing with increasing the CaO loadings, and vice versa with Ce mapping. The d-spacing of the pristine CeO_2 (0.26 nm) lattice planes along with the modified bi-functional catalytic systems are shown in the supplementary information (Figure S1) with values in the range of 0.22-0.26 nm.

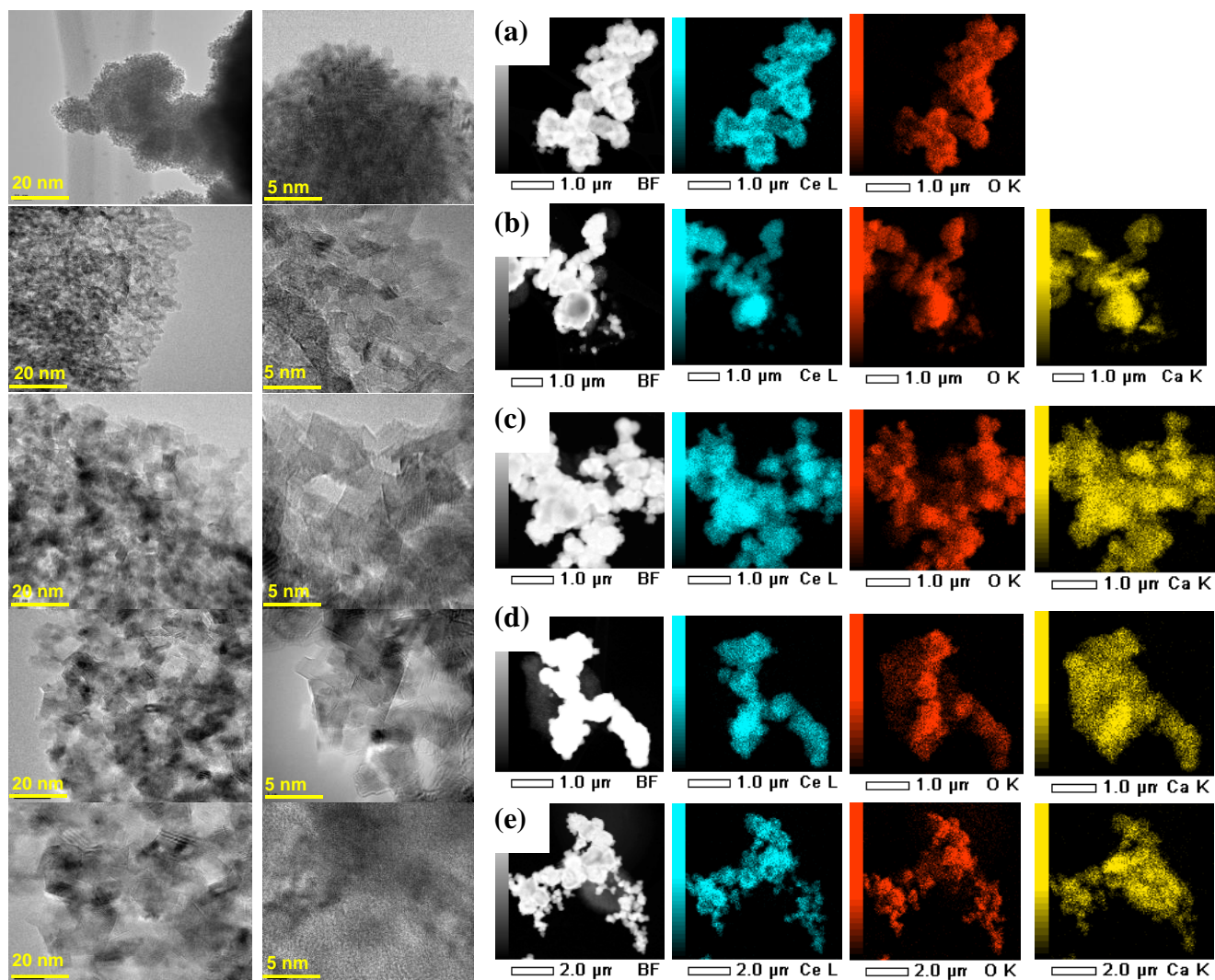


Figure 5: STEM images for CaO/CeO₂ catalysts along with elemental mapping of Ca, O and Ce elements. a) CeO₂ support, (b-e) are 5, 10, 15 and 20 wt. CaO/CeO₂ catalyst, respectively.

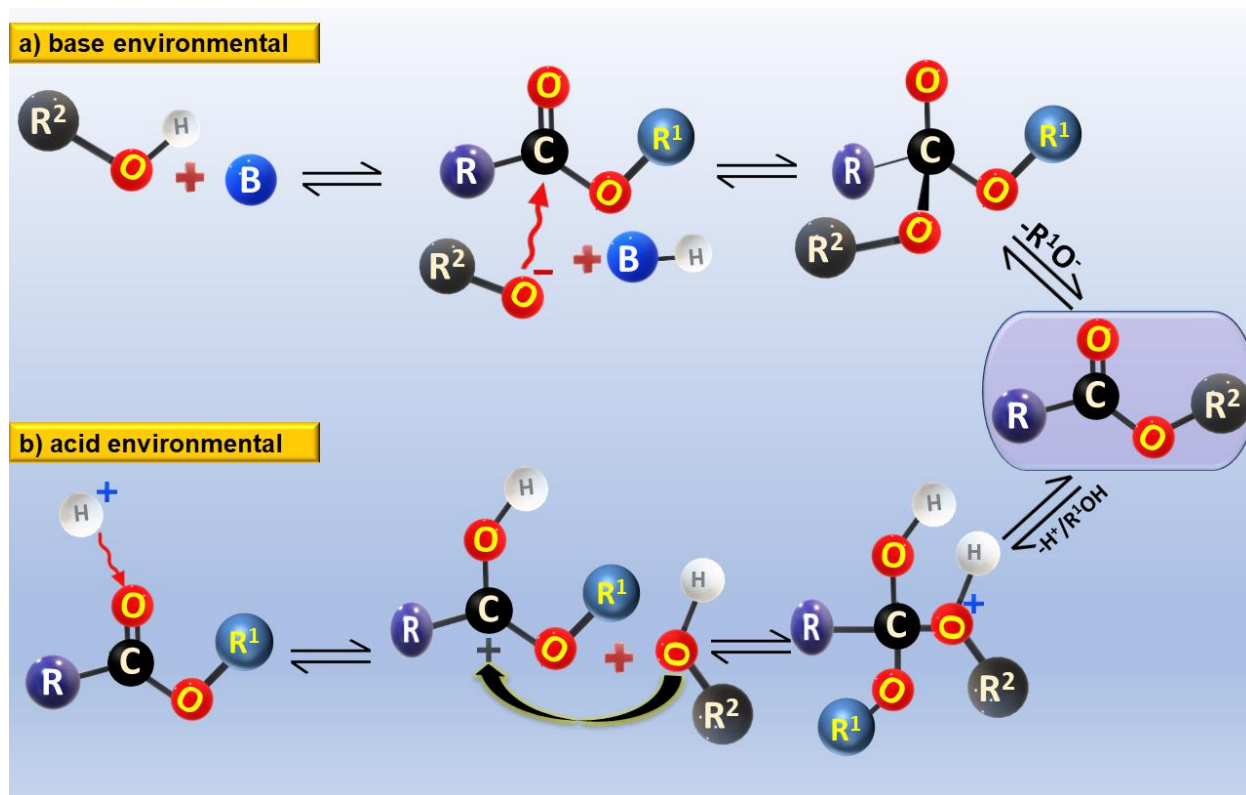
3.2 Catalytic activity

All synthesised catalysts were used for biodiesel production by transesterification to determine the best-modified catalyst herein, which was evaluated based on similar reaction conditions. Such as a temperature of 65 °C, a reaction time of 70 minutes, the molar ratio (methanol: oil) of 6 and 3 wt.% of catalyst was used for the reaction. Biodiesel yield was monitored for all conditions based on all parameters, as shown in Figure 6. The lowest CaO loading, i.e., 5 wt.% CaO-CeO₂ catalyst, showed the lowest biodiesel yield of 46.32 (±0.1) %. This increased to 62.36 (±0.1) % by increasing the CaO loading into 10 wt.% CaO (10 wt.% CaO-CeO₂). The maximum biodiesel yield of 81.32 (±0.1) % was obtained when 15 wt.% CaO-CeO₂ catalyst was used as a catalyst. However, by increasing the CaO loading to 20 wt.% CaO (20 wt.% CaO-CeO₂), the biodiesel yield decreased to 78.26 (±0.1) %. Each experiment was performed thrice in order to reduce the experimental error up to maximum. The highest biodiesel yield herein for 15 wt.% CaO-CeO₂ can be related to several factors, such as it possessed better physicochemical properties. For example, the surface area, pore diameter, and volume provide the proper pore channel to transport reactants and products easily and offer bifunctional active sites to maximise biodiesel yield, as shown in scheme 1. Besides, the high count of smaller particle size (maximum particle count on 250 – 300 nm in diameter), the highest concentration of Ca content (see Figure 3e) as well as specific surface area (see Table 3) amongst the catalysts led to the best performance on biodiesel yield.

Moreover, as shown in elemental mapping, the 15 wt.% CaO-CeO₂ catalyst possessed a uniform material distribution, which can be related to the observation that uniform distribution allowed reactants to react easily and without causing mass transfer limitations in the adsorption of reactants and desorption of products. Thus, to sum up, the catalytic results showed that 15 wt.% CaO-CeO₂

catalyst was the most active catalyst herein for biodiesel production, and it can be used further for parametric studies to obtain optimal operating conditions.

The synthesised catalysts possessed both acidic and basic sites, simultaneously proceeding with both the esterification and transesterification reaction. Due to the presence of high content of FFA determined based on the acid value of oil (5.6 mg of KOH/g of oil), it needs to be pre-treated before transesterification thus due to the nature of the synthesised catalyst, as it possessed both acidic and basic sites, both reactions are expected to proceed simultaneously as shown in Scheme 1. The reaction mechanism can be split into three steps: initially, reactants get adsorbed on the surface of the catalyst, followed by interaction with active sites and in the last stage, desorption of products. For esterification and transesterification, it happens in a way that first anions are formed in the form of a carbocation from FFA and oxygen from methanol followed by the nucleophilic reaction between anions and the carbonyl group of triglyceride and hydroxyl group of methanol and for each present molecule which tends to the occurrence of esterification and transesterification simultaneously. In the last stage, $-OH$ and $-C-O-$ bonds are ruptured, resulting in the formation of products which are mono-alkyl esters and glycerol, followed by their desorption from the catalyst surface and make availability of active sites for the next reaction cycle.



Scheme 1: Shows the mechanistic way in the production of biodiesel either from base or acid environments.

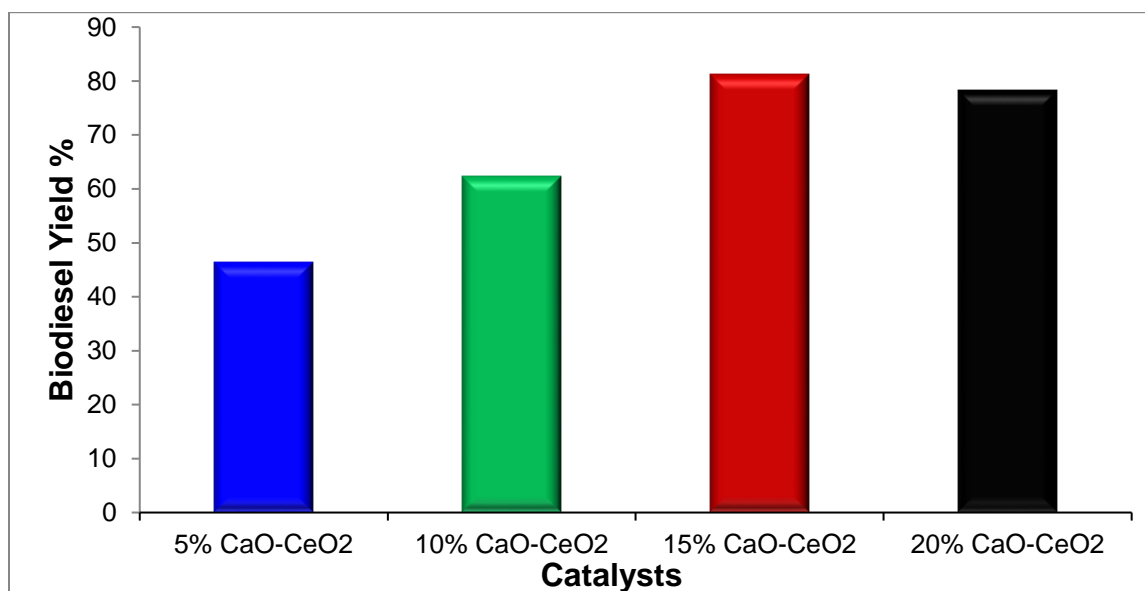


Figure 6: Catalyst evaluation for biodiesel production of 5 wt.% CaO-CeO₂, 10 wt.% CaO-CeO₂, 15 wt.% CaO-CeO₂ and 20 wt.% CaO-CeO₂ catalysts.

3.3 Parametric Studies

To report the feasibility of the synthesised catalysts for the commercial-scale trials, a parametric study is a key aspect to be considered for the economical production of biodiesel. A detailed parametric study was conducted within the range of operating variables, as shown in Table 1. Figure 7 shows the overall behaviour of all parameters concerning the yield of biodiesel. Figure 7a shows the biodiesel yield with respect to temperature; which showed that temperature is quite effective, and it altered the product yield marginally, at 55.36 (± 0.1) %, which is due to reactant molecules (methanol and oil) not being in a much-excited state to react and transform into biodiesel. The rise in the temperature up to 60 °C, a significant increment for biodiesel yield was reported at 84.25 (± 0.1) %. As reported earlier, the temperature tends to increase the kinetic energy of molecules, leading to more effective collisions that help overcome the activation energy required for the reaction. When the temperature was further increased to 70 °C, marginally, the yield of biodiesel increased to 90.14 (± 0.1) %. However, with further increase in temperature, the biodiesel yield slightly decreased to 88.92 (± 0.1) % at 80 °C. Moreover, the lower biodiesel yield at 80 °C is explained by the fact that the reaction temperature is higher than the boiling temperature of methanol, which evaporates into a gas phase; not leaving enough quantity in the liquid phase to react with oil, thus, causing a decrease in biodiesel yield.

While investigating biodiesel production through transesterification, reaction time is an essential parameter to be considered. The residence time effect on the biodiesel yield when a process was carried out in the presence of the most active synthesised novel catalyst is shown in Figure 7b. The time refers to the residence time of reaction, reflecting all parameters such as interaction duration of reactants and the reactants' exposure to active catalyst sites. Figure 7b shows that initially, when the time was low at 30 min, the biodiesel yield was the lowest at 46.84 (± 0.1) %, which reflects

that at this duration, reactant molecules did not have enough time to interact with the active sites of the catalyst properly and the reaction has been stopped, leading to a lower yield of biodiesel. When the temperature was increased to 60 min, the biodiesel yield increased to 79.62 (± 0.1) %. It has been reported earlier and adopted on a commercial scale that biodiesel production's reaction time should be 60 min while using a homogeneous conventional catalyst; however, it varies when a heterogeneous catalyst is used for biodiesel production. As in the case of a heterogeneous catalyst, the reactant molecules get adsorbed onto active sites of the catalyst, and the accessibility of these reaction sites tends to limit the rate of reactions.

Furthermore, when the reaction time was increased to 90 min, biodiesel yield was also increased significantly to 90.14 (± 0.1) %, which can be attributed to the fact that providing enough time, reactant molecules are allowed to interact with the active sites of catalyst, yielding a higher biodiesel yield. Moreover, when the time was further increased to 120 min, the biodiesel yield slightly decreased to 87.39 (± 0.1) %. Thus, it can be concluded that the maximum yield of biodiesel can be obtained when the reaction time was kept to 90 min.

Transesterification is a reversible reaction that involves methanol and oil as reactants resulting in methyl esters known to be biodiesel. So, in order to optimise the process, it is essential to adjust the quantities for methanol and oil to get a better yield of methyl esters. Based on this fact, the molar ratio of methanol to oil was varied within the defined range to get the most suitable quantities for maximum yield, as shown in Figure 7c. Initially, when the methanol to oil molar ratio was kept at 6, the biodiesel yield was the lowest at 71.36 (± 0.1) %; however, when it was increased to 9, the yield increased to 90.14%. The lowest biodiesel yield achieved initially when the ratio was 6 is due to the quantity of methanol, which might not be enough to replace its alkyl group completely with the hydroxyl group to form biodiesel. However, when the methanol to oil ratio increased, the

maximum methyl groups were replaced by the hydroxyl group of oil, leading to higher biodiesel yield. Furthermore, it is observed that when the methanol to oil ratio was further increased to 12 and even to 15, biodiesel yield decreased to 89.00 (± 0.1) and 86.75 (± 0.1), respectively, giving the dome-shaped trend in the plot for the methanol to oil ratio with respect to biodiesel.

Catalyst is an essential part of transesterification in biodiesel production, and its quantity plays a crucial role in the biodiesel yield. Figure 7d shows the effect of catalyst loading concerning biodiesel yield. Initially, when the catalyst loading was 2 wt.%, the biodiesel yield was the lowest at 69.37 (± 0.1) %, while by increasing the catalyst loading to 4 wt.%, the biodiesel yield increased to 90.14%. The cause of low biodiesel yield at 2 wt.% catalyst loading is that the catalyst amount was less in the reaction vessel. The number of active sites contributing to forming the biodiesel was small, which resulted in a lower biodiesel yield. However, when the amount of catalyst was increased, the biodiesel yields increased, leading to the observation that the quantity of active sites of the catalyst is an important aspect as it can change the reaction kinetics.

Furthermore, when the catalyst loading for transesterification was increased further to 6 and 8wt.%, the methyl ester formation decreased to 86.38 and 83.58 (± 0.1)%, respectively. Thus, the low formation of methyl esters is due to the presence of a higher quantity of catalyst in the reaction vessel that might have led to a mass transfer limitation, which disturbed the reaction kinetic and resulted in low product yield. Moreover, a higher amount of heterogeneous catalyst present in the reaction vessel leading to the decrement in biodiesel yield can cause difficulty in mixing, thus ending up with lower product yield.

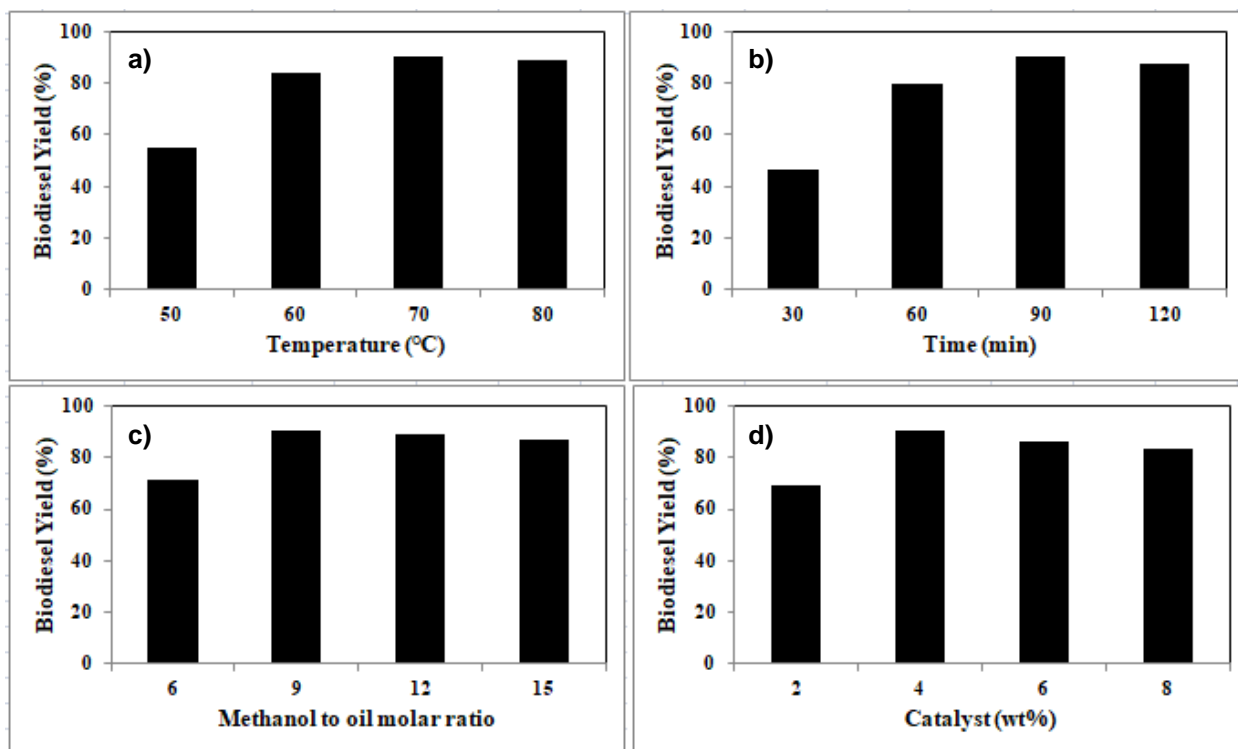


Figure 7: Parametric for biodiesel by using a synthesised novel catalyst

3.4 Quality of Biodiesel

Methyl esters resulting from the transesterification of oil and methanol was characterised by ASTM and EN for their quality. Several important fuel properties were determined as per standards, and their values are mentioned in Table 4, along with standard values for comparison. Acid value (AV) for the produced biodiesel was 0.31 mg KOH/g of oil, and it is less than the limit defined by ASTM and EN standards. The AV measurement of biodiesel produced meant to quantify the presence of FFA within the biodiesel, and if the FFA within biodiesel is high, this will lead to a higher acid value, which results in the corrosive nature of the product biodiesel, causing the difficulty in storage and transportation. So, to have safe storage and transportation AV of biodiesel should be lower than the limit defined by standards. The biodiesel produced herein using the novel catalyst has acid value within limits, so it is safe for storage and transportation. The

biodiesel density was 899 kg/m^3 and it is within the limit defined by the EN standard. As density refers to mass per unit volume for biodiesel to have economical consumption of biodiesel when used as fuel, it is compulsory to have a lower density and within the international standard limit. The kinematic viscosity (KV) produced biodiesel was $3.98 \text{ mm}^2/\text{s}$, satisfying both ASTM and EN standards. Viscosity is directly related to fuel efficiency for the engine as the fuels with a higher viscosity may lead to atomisation when injected for combustion; however, less viscous fuels are suitable for proper combustion and to have better engine efficiency. So, when referring to fuel production, it is important to control and manage the viscosity of the fuel.

The water content (WC) in the produced biodiesel was almost negligible ($0.01 \text{ vol}\%$), which means that the biodiesel would be suitable for combustion in the engine without causing any lag. The energy density, also known as the calorific value (CV), was 43.28 MJ/kg . The calorific value of producing biodiesel is almost similar to fossil diesel ($44.36 - 46.21 \text{ MJ/kg}$), reflecting that the produced biodiesel can give a similar engine efficiency when combusted compared to fossil-based fuels. The major issue in the commercialisation of biodiesel is its poor low-temperature properties, which are cloud, pour and cold filter plugging point. These properties depend on the composition of biodiesel. The biodiesel reported in current research had better low-temperature properties such as cloud point (CP) was $1.1 \text{ }^\circ\text{C}$, pour point (PP) $-3.2 \text{ }^\circ\text{C}$ and cold filter plugging point (CFPP) $-1.7 \text{ }^\circ\text{C}$. Measured low-temperature properties lead to the observation that the biodiesel produced herein is also suitable for colder regions and can be used as fuel without any discrepancy. The Flash point (FP) of diesel or biodiesel refers to the maximum temperature that it can sustain without catching fire. The flash point for producing biodiesel was $167 \text{ }^\circ\text{C}$, reflecting that this biodiesel can be easily stored and transported. Cetane number refers to the anti-knocking property of biodiesel; thus, for the produced biodiesel, it was 62.35 , which is higher than the minimum limit defined by ASTM

and EN standards. The quantity of glycerin (free glycerin (FG) and total glycerin (TG)) was also less than the maximum values given by standards. Thus, based on all measured properties of produced biodiesel, it can be concluded that it satisfies all standards and could be used as potential alternative fuel instead of fossil diesel from a novel Loquat seeds oil.

Table 4: Fuel properties for produced biodiesel and comparison with the standard values

Property	Biodiesel	ASTM 6751	EN 14214
Density (kg/m ³) @ 25 °C	899	- ^a	860-900
AV (milligram of KOH/gram of oil)	0.31	0.50 max	0.50 max
CN	62.35	47 min	51 min
CP (degree Celsius)	1.1	Report	- ^b
PP (degree Celsius)	-3.2	- ^a	- ^b
FP (degree Celsius)	167	93 min	120 min
FG (percent)	0.019	0.020 max	0.020 max
TG (percent)	0.236	0.240 max	0.250 max
KV (mm ² /s) @ 40 degree Celsius	3.98	1.9-6.0	3.5-5.0
WC (volume percent)	0.01	0.05	- ^a
CV (Megajoule/kilogram)	43.28	- ^a	- ^a
CFPP (degree Celsius)	-1.7	- ^a	- ^b
Sulphur content	0.032	15 mg/kg max	10 mg/kg max

3.5 Reusability of catalyst

To commercialise the catalyst for biodiesel production, it is important to determine the reusability of the catalyst. The reusability of the catalyst is also referred to as economising the process and

reducing the product cost. Consequently, the reusability of synthesised catalysts (15 wt.% CaO-CeO₂) was measured for biodiesel production, as shown in Figure 8. The used catalyst was washed thoroughly with hexane to remove any kind of product and by-product, then calcined and reused for the experimental run. When the catalyst was calcined and reused, the biodiesel yield was almost the same $\pm 0.5\%$; however, when biodiesel production was used without calcination, the biodiesel yield was reduced by 15%.

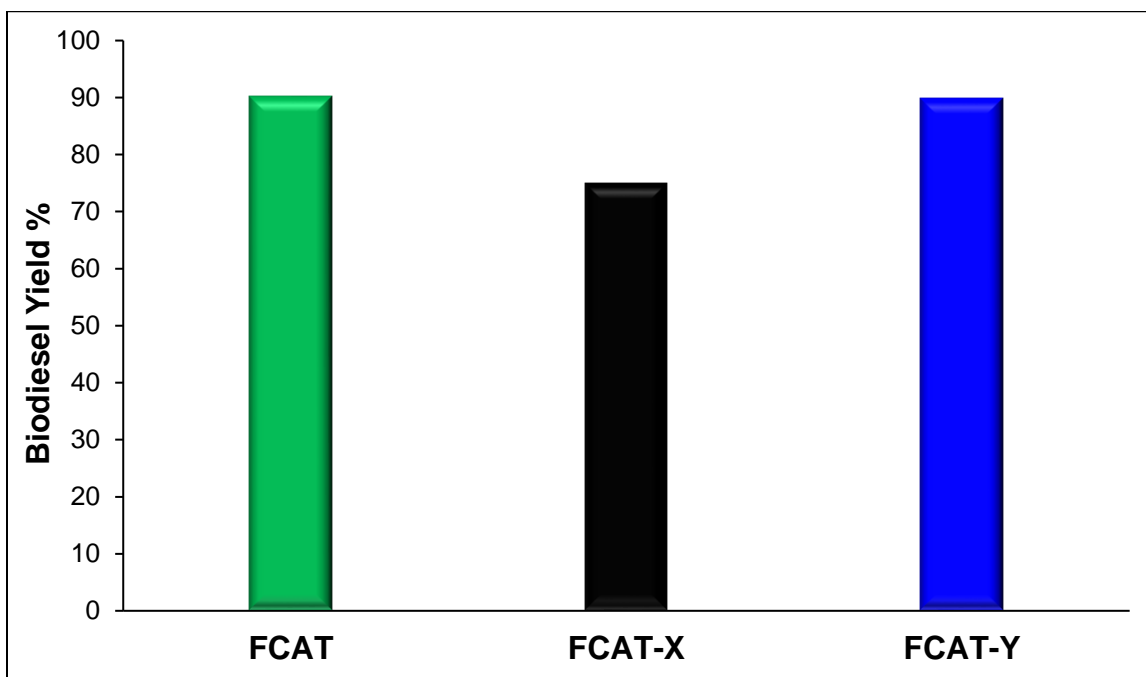


Figure 8: Reusability of synthesised catalyst where FCAT (fresh 15 wt% CaO-CeO₂), FCAT-X (used catalyst without regeneration 15 wt% CaO-CeO₂) and FCAT-Y (used catalyst with regeneration 15 wt% CaO-CeO₂)

This shows that the physicochemical properties of the spent catalyst and yields were not much affected after calcination; however, when the catalyst was used without regeneration, the surface area and pore volume were decreased, as shown in Table 5. Thus, this observation leads to the fact that when the used catalyst is regenerated, the active sites are readily available for a reaction similar

to the fresh catalyst. However, when the catalyst is not regenerated, the active sites are blocked by unwanted material, causing biodiesel yield decrement. Thus, it can be concluded that upon each reuse, the catalyst needs to be regenerated to get a higher yield of biodiesel.

Table 5: BET analysis for reusability studies where FCAT (fresh 15 wt% CaO-CeO₂), FCAT-X (used catalyst without regeneration 15 wt% CaO-CeO₂) and FCAT-Y (used catalyst with regeneration 15 wt% CaO-CeO₂)

Catalyst	Specific surface area (m ² /g)	Pore volume (cm ³ /g)	Pore diameter (nm)
FCAT	39.65	0.51	7.87
FCAT-X	28.32	0.43	7.19
FCAT-Y	39.64	0.51	7.81

3.6 Life cycle assessment

This study set out to investigate the usability of loquat seeds waste to produce biodiesel. The methods followed included preparing CaO/CeO₂ catalyst and determining the appropriate wt% of catalyst to achieve maximum efficiency for converting loquat seed oil to biodiesel. The later part of the study conducted a life cycle assessment to determine the environmental impacts of the process.

The goal of using LCA in the current study is to evaluate the environmental and human health impacts of biodiesel products from loquat seed oil, considering the guidelines provided by ISO: 14040 and ISO: 14044. The LCA enables scientists, practitioners and decision-makers to understand the damage to the environment, human health and resources due to the use of raw materials and emissions over the entire production chain [38, 46].

The LCA conducted in this study had a cradle-to-gate attributional approach and excluded environmental impacts due to infrastructure processes. The functional unit in this study is 1000 kg of biodiesel produced using waste loquat seeds as raw material. The system boundary for the LCA consisted of: (1) Raw material transportation of waste loquat seeds from farms to oil extraction centre, (2) Oil extraction from waste loquat seeds, (3) Catalyst preparation using $\text{Ca}(\text{NO}_3)_2 \cdot 4\text{H}_2\text{O}$ and $\text{Ce}(\text{NO}_3)_2 \cdot 6\text{H}_2\text{O}$ and regeneration using hexane, and (4) biodiesel production via transesterification utilising catalyst and methanol (Figure 9). The waste products from the system included gaseous emissions, wastewater and solid cake, for which treatment processes were not considered part of the system boundary.

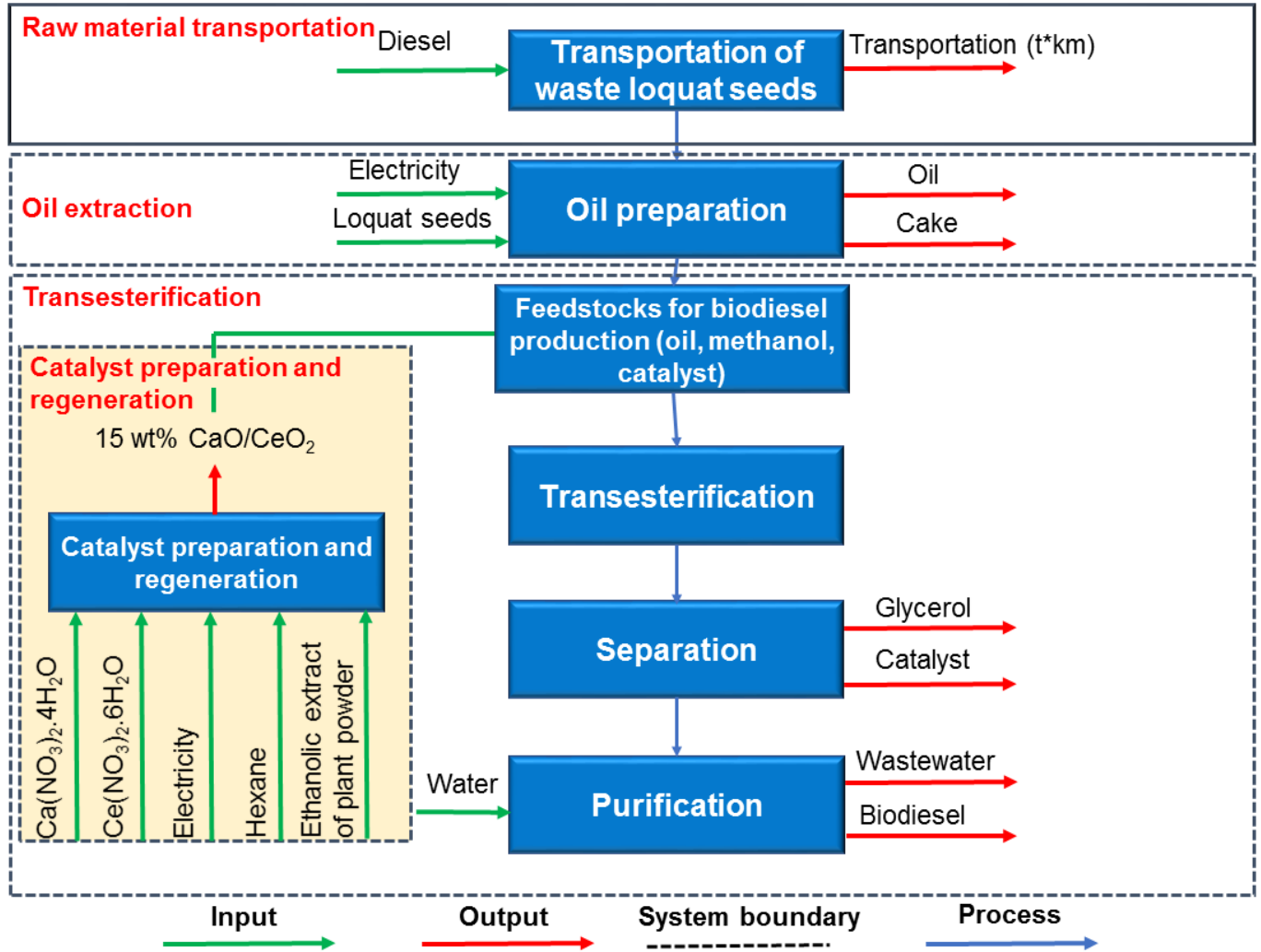


Figure 9: System boundary for life cycle analysis of biodiesel production using waste loquat seeds.

[t*km represents tonne*transportation distance in km]

3.6.1 Inventory analysis

The raw material transportation for 200 km was considered in the present study from farms to the oil extraction centre for loquat seeds (Table 6). Moreover, the production of loquat seeds was not considered part of the system boundary, as currently, these seeds are not used for any major application and are an abundant waste source. Although the present study used a soxhlet method

of loquat seed oil production, it has been studied that large-scale production applying soxhlet extraction can lead to high consumption of solvents [50]. Consequently, it was considered that oil extraction would be carried out in oil mills with an efficiency of 10%. This is to account for a realistic scenario in which large scale production of biodiesel would also reflect in large scale production of loquat seeds oil. The energy required for screw-type press and pumps was referred from Fridrihsone et al. [47].

In addition to biodiesel production using loquat seed oil, catalyst preparation and regeneration were also considered part of the subsystem for LCA. It was observed that the best yield of biodiesel was at 4 wt.% catalyst in the transesterification reaction. Accordingly, for producing 1000 kg of biodiesel, 3.6 kg of catalyst is required, which would be regenerated after every transesterification reaction for a total of 18 cycles. This is in line with the study from Thitsartarn and Kawi [48], which showed that the CaO/CeO_2 catalyst could be used for a total of 18 cycles. The catalyst had high reactivity at 15 wt.% CaO/CeO_2 ; thus, the weight required for $\text{Ca}(\text{NO}_3)_2 \cdot 4\text{H}_2\text{O}$ and $\text{Ce}(\text{NO}_3)_2 \cdot 6\text{H}_2\text{O}$ are 2.35 kg and 6.8 kg, respectively, for preparing 3.6 kg of catalyst. To carry out the mixing of chemicals used in the process, an electric mixer was used, and the energy required was calculated using the equipment operating power consumption [49]. The electrical energy required for the industrial autoclave to maintain the temperature at 180 °C was referred from [50]. After every cycle, hexane consumption was considered 1 L for 1 kg of catalyst and electrical power consumption for calcination was calculated using instrument operating conditions [51].

The location of the catalyst preparation plant was assumed to be in proximity with the biodiesel production plant; therefore, transportation distance between catalyst preparation plant to biodiesel production plant was not considered in the LCA. Moreover, in the overall stage of biodiesel production, there are stages such as transesterification. The feedstocks for transesterification

included methanol, catalyst and loquat seed oil. The experiments showed the use of methanol: oil as 9:1 and 4 wt.% of catalyst. The required energy for carrying out transesterification was referred from Mohammadi et al.[52] This concluded the use of 32 kWh of electricity for carrying out the biodiesel production process in a quantity of 1000 kg from palm oil.

At the end of the reaction, the amount of catalyst was assumed to be constant with no catalyst consumption in the reaction. The reaction output from the present study reflected an efficiency of 90.14% conversion from loquat seeds oil to biodiesel. Thus, 1232.6 kg of loquat seed oil along with 0.36 kg of catalyst for 18 cycles and 40.67 kg of methanol leads to glycerol production (475.5 kg) and biodiesel (1000 kg) considering losses due to separation. During the separation of glycerol from the biodiesel mixture, 90% efficiency was assumed [53]. A 1 m³ of warm water was assumed to use to purify the biodiesel mixture. The output of the wastewater generated during the process was assumed at 10% loss due to evaporation during the separation process, in line with the work of Photaworn et al. [54]. The biodiesel produced showed a calorific value of 43.28 MJ/kg, thus producing fuel with 43280 MJ.

Table 6: Inventory analysis for conducting LCA of production of 1000 kg of biodiesel using waste loquat seeds.

Inventory item	Unit	Input	Output	Reference
Raw material transportation				
Diesel	kg			
^a Transportation (tractor)	tkm		2465.2	Calculation (t*km)
Loquat seed oil extraction				
Loquat seeds	kg	12326		
^b Electrical energy for pressing oil	kWh	313.2		[47]
Electrical energy for pumping oil	kWh	1.44		[47]
Loquat seed oil	kg		1232.6	

Solid cake	kg		10846.9	
Loss	kg		246.52	
Catalyst preparation and regeneration for use for a total of 18 cycles				
Catalyst preparation				
Electricity required for mixing	kWh	10		Instrument -
Water	L		3.6	[54]
Plant powder for ethanolic extract	g	91.5		
Ethanol (10% v/v)	L	915		
Ca (NO₃)₂·4H₂O	kg	2.35		
Ce (NO₃)₂·6H₂O	kg	6.8		
Electrical energy for autoclave	kwh	516		Instrument operating [50]
Catalyst	kg		3.6	
Wastewater	L		826.74	
Catalyst regeneration for 17 more cycles				
Hexane	L	65.5		Calculations based on Section 3.5
Electrical energy for calcination	kwh	68		Instrument operating [51]
Wastewater	L		59.9	
Biodiesel production				
Electrical energy for transesterification	kWh	35.5		[52]
Warm water	L	1000		[52]
Methanol	kg	406.7		
Glycerol	kg		475.5	
Loquat seeds oil	kg	1232.6		
Separation losses (10% of glycerol and biodiesel)		211.6		[53]
^c Biodiesel	kg		1000	

Wastewater	L	900		[54]
-------------------	---	-----	--	------

^a *Transportation: Lorry transport, Euro 0, 1, 2, 3, 4 mix, 22 t total weight, 17,3 t max payload RER (SimaPro 8.0 LCA database)*

^b *Electricity, production mix PK (WFLDB 3.1)/PK U (SimaPro 8.0 LCA database)*

^c *Biodiesel calorific value: 43.28 MJ/kg (biodiesel characterisation in this study, Section 3.4)*

3.6.2 Midpoint indicator assessment

In this study, the midpoint indicator assessment was conducted based on the CML-IA baseline V3.06 method, using SimaPro 8.0 to better understand and compare the impact categories. Table 7 shows the midpoint indicator assessment results for various environmental, human health and resource impacts for single environmental problems. Abiotic depletion corresponds to the depletion of fossil fuels, minerals, clay and peat and represented as kg antimony equivalent (kg Sb eq), abiotic depletion of fossil fuels is related to extraction of fossil deposits, global warming potential (GWP 100a), is evaluated for a time horizon of 100 years, ozone layer depletion (ODP) was accounted for a time scale of 40 years [55], human toxicity is an index that corresponds to potential harm of a unit of chemical released into the environment, and is based on both the inherent toxicity of a compound and its potential dose [56], environmental toxicity is calculated in three separate categories which examine damage to terrestrial, freshwater and marine sources for the entire production process, photochemical oxidation refers to emissions of reactive substances injurious to human health and ecosystems, acidification is caused by the emission of acidifying substances, and finally, eutrophication consists of the effect of releasing excessive amount of nutrients.

Table 7. Environmental impacts due to production of 1000 kg of biodiesel from waste loquat seed oil.

Impact category	Unit	Raw material transportation	Oil extraction	Catalyst preparation and ^a regeneration	Transesterification
Abiotic depletion	kg Sb eq	0.000	0.000	0.003	0.000
Abiotic depletion (fossil fuels)	MJ	1137.841	1021.489	8531.971	15657.487
Global warming (GWP100a)	kg CO ₂ eq	81.232	103.745	402.285	541.323
Ozone layer depletion (ODP)	kg CFC-11 eq	0.000	0.000	0.000	0.000
Human toxicity	kg 1,4-DB eq	2.541	50.017	211.607	157.551
Fresh water aquatic ecotox.	kg 1,4-DB eq	0.041	67.446	173.519	44.981
Marine aquatic ecotoxicity	kg 1,4-DB eq	1085.254	198040.184	917860.498	174943.453
Terrestrial ecotoxicity	kg 1,4-DB eq	0.003	0.147	0.475	0.039
Photochemical oxidation	kg C ₂ H ₄ eq	0.028	0.019	2.484	0.164
Acidification	kg SO ₂ eq	0.383	0.574	1.744	2.604
Eutrophication	kg PO ₄ ³⁻ eq	0.088	0.434	1.306	0.084

^a Catalyst was used for a total of 18 cycles.

Calculations were based on the CML-IA baseline V3.06 method

Considering cumulative environmental impacts, raw material transportation caused the least environmental impacts. This is due to the distance consideration of 200 km in the present study. Similar findings were recorded by Chung et al. [53] for the production of biodiesel from waste cooking oil.

For raw material preparation, which included extraction of loquat seed oil from waste loquat seeds, marine aquatic ecotoxicity as 190840 1,4-DB eq (kg 1,4 dichlorobenzene equivalent), depletion of fossil fuels as 1021 MJ and global warming potential as 104 kg CO₂ eq were observed. This is due to the high electricity input for the screw press and oil pump.

The catalyst preparation and regeneration stage showed marine aquatic ecotoxicity as 917861 kg 1,4-DB eq, depletion of fossil fuels as 8532 MJ and global warming potential as 403 kg CO₂ eq. The catalyst was considered to be used for a total of 18 cycles after cleaning using hexane and regeneration using calcination after every cycle.

The final stage evaluated for LCA was biodiesel production using the transesterification process. It was recorded that this stage showed the highest environmental impacts in terms of global warming potential and depletion of fossil fuels, which could be due to the electricity requirement for transesterification and chemical inputs such as methanol. The cumulative abiotic depletion of fossil resources over all the processes was 26349 MJ, global warming potential as 1129 kg CO₂ eq, and human health toxicity as 422 kg 1,4-DB eq (Table 7).

Relative results depicting the contribution of each step in the production chain were generated from the simulation, in which indicator results maximum is set 100%. Each impact is standardised with the value of the worst scenario for this impact. Figure 10 shows that catalyst preparation and regeneration is mostly above all other processes in terms of impact categories. This is due to the larger amount of carbon dioxide being produced during the preparation and reaction of Ca (NO₃)₂.4H₂O and Ce (NO₃)₂.6H₂O. The raw material transportation contributed the least to environmental impacts. The last stage involving biodiesel production using transesterification contributes to electrical energy and methanol, resulting in the highest abiotic depletion of fossil fuels, global warming potential, and acidification.

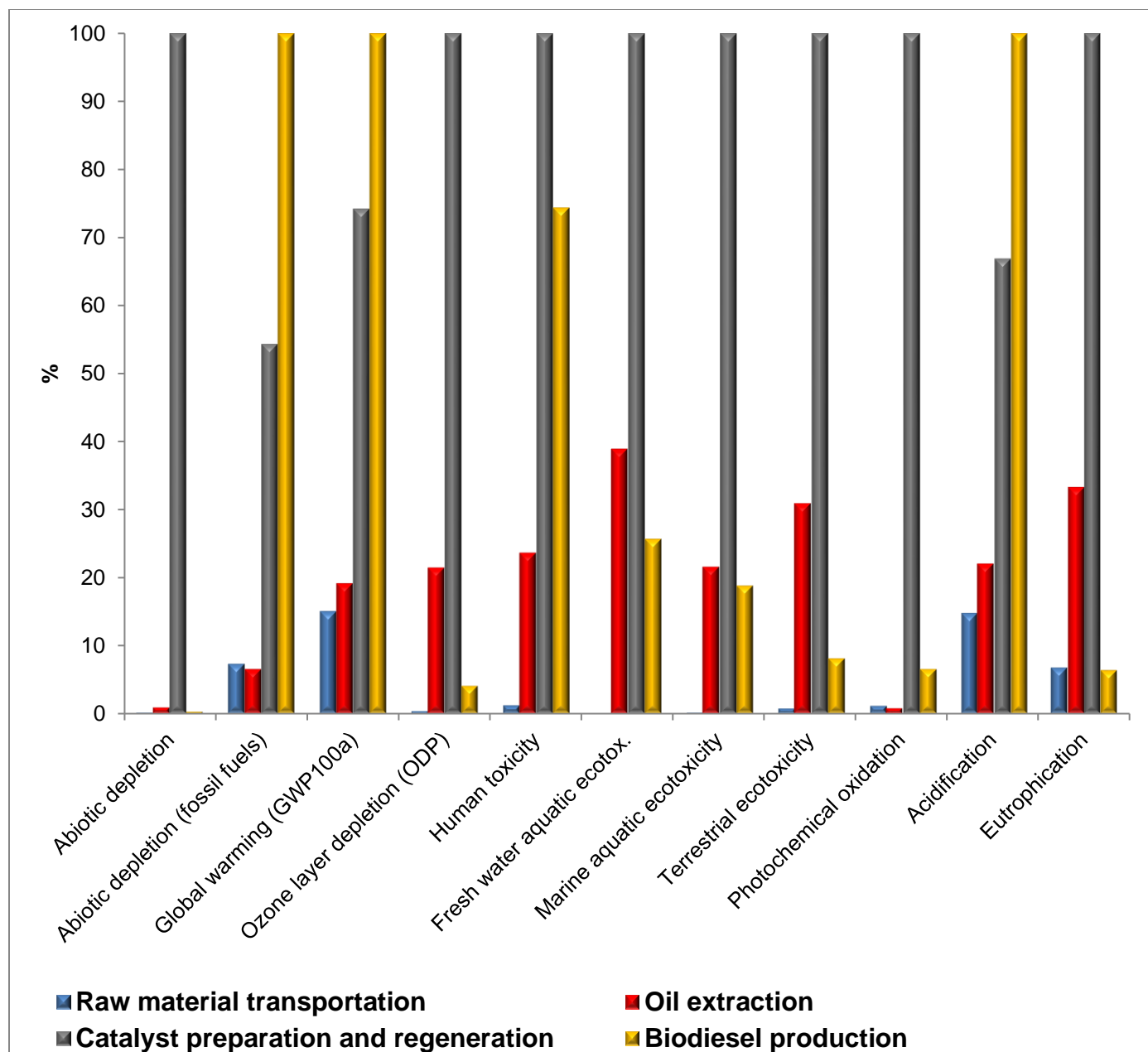


Figure 10: CML-IA baseline V3.06 midpoint indicators for 1000 kg of biodiesel production from loquat seed oil using CaO/CeO₂ catalyst.

[Catalyst was used for a total of 18 cycles.]

3.6.3 Endpoint indicator assessment

ReCiPe 2016 Endpoint (E) V1.04 was used to conduct endpoint analysis. Table 8 shows the endpoint indicator assessment for the production chain from the transportation of waste loquat seeds to the conversion of oil to biodiesel. Endpoint indicators aggregate the single midpoint indicators, to simplify the interpretation of LCA findings as human health, ecosystem quality and resources: (1) Human health is related to the impacts of environmental degradation that results in an increase of and duration of loss-of-life-years due to ill health, disability or early death and is recorded as DALY (Disability-adjusted life year), (2) Ecosystem quality is linked to the impact of global warming potential, ozone layer depletion, acidification, ecotoxicity, eutrophication and indicates biodiversity loss. It is recorded as local species loss integrated over time (species * yr), and (3) For resources, it is closely related to the depletion rate of raw materials and energy sources. It is in US dollars (\$), representing the extra costs involved for future mineral and fossil resource extraction. Agricultural resource depletion was not considered in the present study, as loquat seeds do not require plantation due to their origin being a waste source.

Table 8: Endpoint indicator impacts due to the production of 1000 kg of biodiesel from waste loquat seeds.

Damage category	Unit	Raw material transportation	Oil extraction	Catalyst preparation and ^a regeneration	Biodiesel production
Human health	DALY	0.001	0.010	0.027	0.008
Ecosystems	species.yr	2.2×10^{-6}	6.3×10^{-6}	19.7×10^{-6}	12.6×10^{-6}
Resources	USD2013	11.18	4.70	71.48	26.80

^a Catalyst was used for a total of 18 cycles.

Calculations were based on ReCiPe 2016 Endpoint (E) V1.04 method.

These endpoints can be further normalised for each impact category (usually by external normalisation) and multiplied by a weighting factor in order to obtain overall environmental

performance indicators in the form of one dimensionless single indicator (a so-called single score) indicated as Point in Figure 11 [57]. This weighting factor expresses the relative importance of the impact category. The weighted results all have the same unit and can be added up to create one single score for the environmental impact of a product or scenario. The findings obtained from the endpoint impact assessment are in accordance with the midpoint indicator impact assessment. With transportation being the lowest contributor to environmental impacts. While catalyst preparation and regeneration contributed to the highest impacts as human health (119.2 Pt) and ecosystems damage (9.3 Pt) and resources (0.5 Pt).

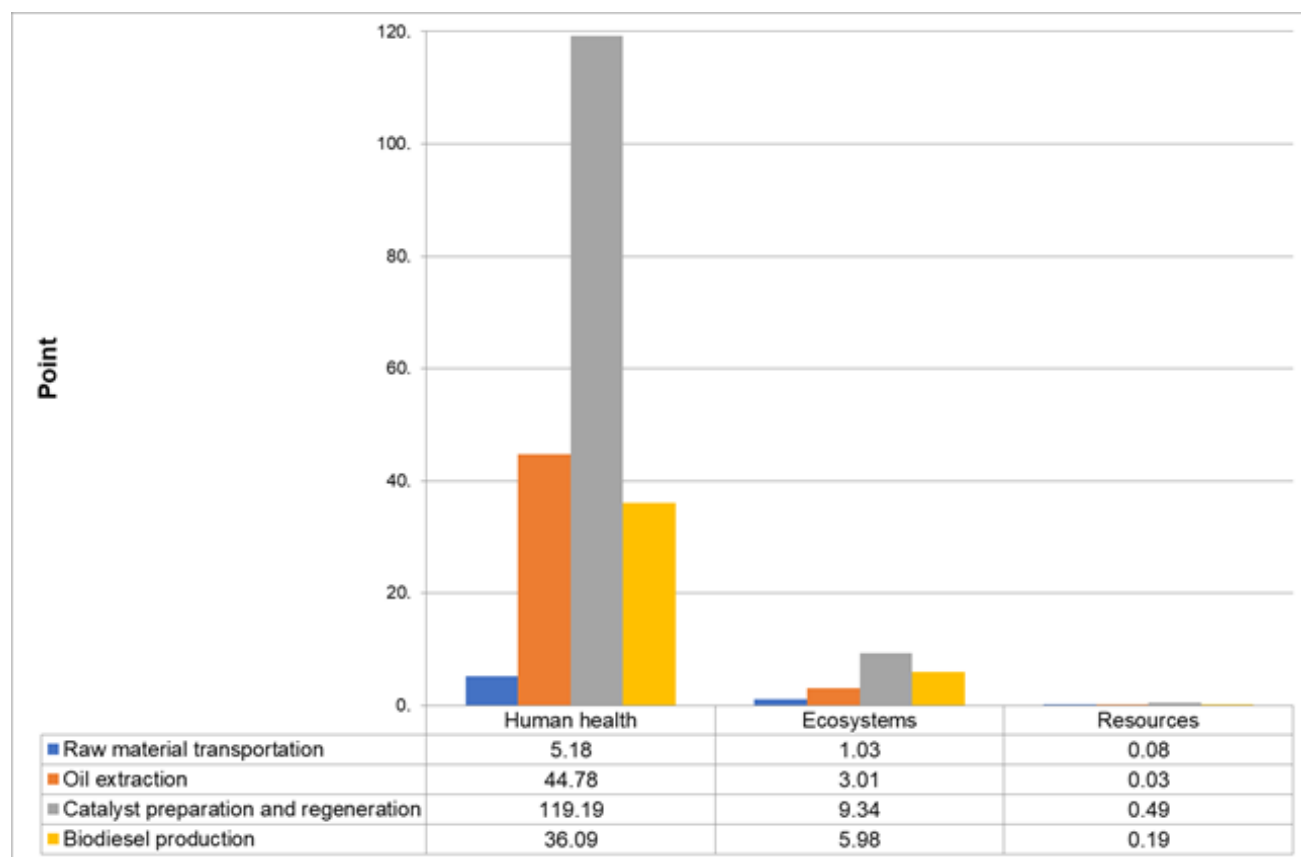


Figure 11: ReCiPe 2016 Endpoint (E) V1.04 endpoint indicators for producing 1000 kg of biodiesel from loquat seed oil using CaO/CeO₂ catalyst.

[Catalyst was used for a total of 18 cycles.]

3.6.4 Sensitivity analysis

To further improve the understanding of the contribution of each process in the entire production chain on individual environmental impacts, a sensitivity analysis was conducted. This was to identify which process of the biodiesel production life cycle contributed directly to the burdensome environmental footprints. Relatedly, if impacts in environmental categories are to be minimised, these will be the processes where future research and development should focus [58]. This sensitivity analysis is presented as Tornado plots in Figure 12 and Supplementary material: S2. The magnitude of each bar refers to the % difference in output associated with a 10% change in single input from its base value. Changes in output linked to an increase in input values are shown in red colour, and output changes due to decrease are represented as blue colour. For example, a 10% increase in catalyst dosing for each cycle could increase 9.88% of abiotic depletion for the entire process. Figure 3 shows that catalyst dose drives the photochemical oxidation impacts strongly. On the other hand, it also reflects that to make the entire process contribute least to abiotic depletion of fossil fuels and global warming potential, greater attention is required for optimising chemicals and electrical energy.

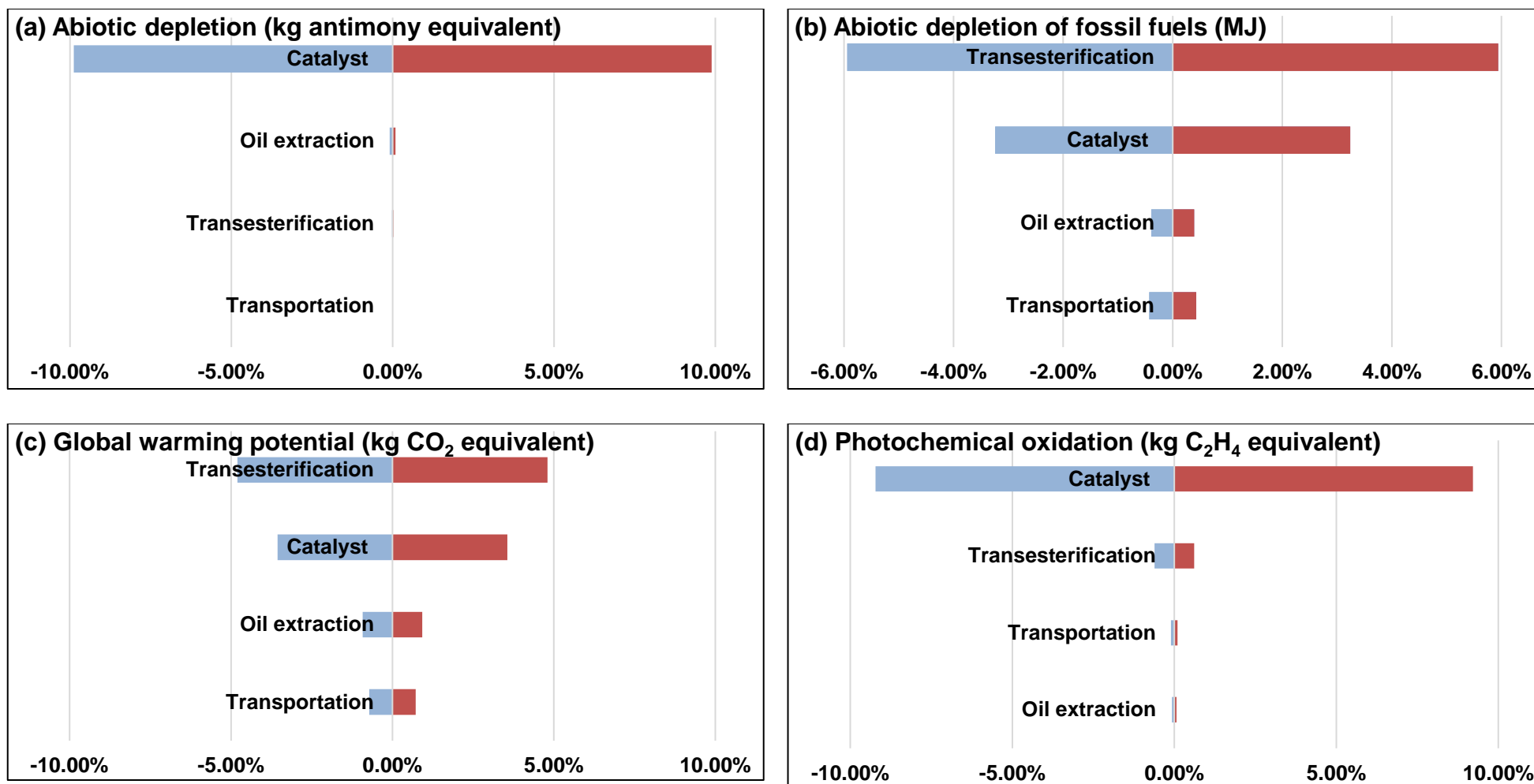


Figure 12: Tornado plots representing the magnitude to which impact in environmental categories such as abiotic depletion, abiotic depletion of fossil fuels, global warming potential and photochemical oxidation are sensitive to a $\pm 10\%$ change in input parameters. For example, if all the input quantities required for transesterification increase by 10%, there will be an increase in global warming potential by 4.8%.

3 *[Catalyst refers to catalyst preparation and regeneration for use for a total of 18 cycles.]*

4 *3.6.5 Implications*

5 The findings recorded in Section 3.6.2. showed that the cumulative abiotic depletion of fossil
6 resources over all the processes was 26349 MJ, global warming potential as 1129 kg CO₂ eq (Table
7 7) to produce 1000 kg of biodiesel. The calorific value of biodiesel is 43.28 MJ/kg, which shows
8 that the net energy output from the process is 43280 MJ. Moreover, glycerol obtained as a co-
9 product from transesterification in a 477.5 kg quantity can be used as soap. This could avoid the
10 depletion of additional 15579 MJ. Therefore, considering the saving of fossil fuel resources due to
11 both biodiesel and soap (glycerol), the net energy ratio is 2.23.

12 It should also be noted that solid cake from the oil extraction process was not considered a co-
13 product for its use as animal feed. This is because the current study did not involve characterisation
14 of solid cake and its protein content, thus usability as animal feed. Future research should analyse
15 the use of loquat seed oil cake for its use as a co-product, which could mitigate the environmental
16 impacts of this stage. Relatedly, the use of solid cake from rapeseed oil was included in LCA of
17 oil production by Fridrihsone et al. [47].

18 In summary, the present study highlighted that the synthesised novel catalyst is highly suitable for
19 biodiesel production from bio-oil derived from nonedible loquat seeds. Moreover, the synthesised
20 catalyst was highly stable based on the reusability studies done. The product biodiesel from
21 nonedible feedstock has potential fuel properties. This shows that agricultural waste feedstocks
22 such as waste loquat seeds can provide alternative fuels.

23 4. Conclusions

24 A highly active bifunctional catalyst has been synthesised herein and used to produce biodiesel
25 from a novel waste source of oil (loquat seed oil). Different loadings of CaO on the ceria oxide
26 support from 5 to 20 wt.% were tested for biodiesel production. Parent material CeO₂ possesses
27 the lowest overall quantities of basic and acidic active sites, with values of 0.098 and 0.077
28 mmol/g, respectively, compared to 2-3 mmol/g for the modified catalysts. The 15 wt.% CaO/CeO₂
29 catalyst showed better surface morphology, bifunctional active sites and a synergistic effect
30 between the nanoparticles of CaO and the CeO₂ support. The optimum biodiesel yield obtained
31 via the parametric study was 90.14 wt.% for the most active bifunctional catalyst (15 wt.%
32 CaO/CeO₂). Where the optimum parameters were set at a temperature of 70 °C, methanol: oil of
33 9, time of 90 minutes and 4 wt.% of catalyst. The reusability of the most active bifunctional catalyst
34 was assessed and showed that it is reusable after the regeneration process with almost the same
35 activity. Finally, the produced biodiesel was investigated as per the standard values given by
36 ASTM and EN, showing that it met all the standard values and further strengthened its potential
37 as an alternative fuel source to be used in a diesel engine without further modifications.

38 The LCA results using midpoint indicators from the CML-IA baseline V3.06 method showed that
39 for the entire process, the cumulative abiotic depletion of fossil resources was 26349 MJ, human
40 health toxicity was 422 kg 1,4-DB eq (kg 1,4 dichlorobenzene equivalent), and global warming
41 potential was 1129 kg CO₂ eq. The highest damage in the majority of environmental categories
42 was observed during catalyst preparation and regeneration. The cumulative end point indicators
43 (ReCiPe 2016 Endpoint (E) V1.04) for human health, ecosystems and resources impact over all
44 the processes were observed as 205.2 Pt, 19.4 Pt, and 0.8 Pt, respectively. Furthermore, the energy

45 ratio (computed as output energy/input energy) was 2.23 by considering allocation of output
46 energy due to biodiesel and glycerol.

47 **Acknowledgement**

48 The authors would like to thank Petroleum Development Oman (PDO) for their generous financial
49 support under grant number CR/SCI/BIOL/18/01. AO and DR would like to acknowledge the
50 support given by of The Bryden Centre project (Project ID VA5048) which was awarded by The
51 European Union's INTERREG VA Programme, managed by the Special EU Programmes Body
52 (SEUPB), with match funding provided by the Department for the Economy in Northern Ireland
53 and the Department of Business, Enterprise and Innovation in the Republic of Ireland. Dr Ahmed
54 Osman and Prof. David Rooney would like to acknowledge the support given by the EPSRC
55 project "Advancing Creative Circular Economies for Plastics via Technological-Social
56 Transitions" (ACCEPT Transitions, EP/S025545/1). The authors would like to thank Charlie
57 Farrell, who assisted in the proof-reading of the manuscript.

58 **Disclaimer**

59 The views and opinions expressed in this paper do not necessarily reflect those of the European
60 Commission or the Special EU Programmes Body (SEUPB).

61 **5. References:**

- 62 [1] F.S. Mirhashemi, H. Sadrnia. NOX emissions of compression ignition engines fueled with various
63 biodiesel blends: A review. *Journal of the Energy Institute*. 93 (2020) 129-51.
64 [2] M. Rehfeldt, E. Worrell, W. Eichhammer, T. Fleiter. A review of the emission reduction potential of fuel
65 switch towards biomass and electricity in European basic materials industry until 2030. *Renewable and*
66 *Sustainable Energy Reviews*. 120 (2020) 109672.
67 [3] S. Sahani, T. Roy, Y.C. Sharma. Studies on fast and green biodiesel production from an indigenous
68 nonedible Indian feedstock using single phase strontium titanate catalyst. *Energy Conversion and*
69 *Management*. 203 (2020) 112180.

70 [4] A.I. Osman, N.C. Skillen, P.K.J. Robertson, D.W. Rooney, K. Morgan. Exploring the photocatalytic
71 hydrogen production potential of titania doped with alumina derived from foil waste. *International*
72 *Journal of Hydrogen Energy*. (2020).

73 [5] A.I. Osman, M. Hefny, M.I.A.A. Maksoud, A.M. Elgarahy, D.W. Rooney. Recent advances in carbon
74 capture storage and utilisation technologies: a review. *Environmental Chemistry Letters*. (2020).

75 [6] M.K. Yesilyurt, M. Aydin. Experimental investigation on the performance, combustion and exhaust
76 emission characteristics of a compression-ignition engine fueled with cottonseed oil biodiesel/diethyl
77 ether/diesel fuel blends. *Energy Conversion and Management*. 205 (2020) 112355.

78 [7] M. Morgenstern, J. Cline, S. Meyer, S. Cataldo. Determination of the Kinetics of Biodiesel Production
79 Using Proton Nuclear Magnetic Resonance Spectroscopy (¹H NMR). *Energy & Fuels*. 20 (2006) 1350-3.

80 [8] U. Jamil, A. Husain Khoja, R. Liaquat, S. Raza Naqvi, W. Nor Nadyaini Wan Omar, N. Aishah Saidina
81 Amin. Copper and calcium-based metal organic framework (MOF) catalyst for biodiesel production from
82 waste cooking oil: A process optimisation study. *Energy Conversion and Management*. 215 (2020) 112934.

83 [9] Y. He, B. Zhang, S. Guo, Z. Guo, B. Chen, M. Wang. Sustainable biodiesel production from the green
84 microalgae *Nannochloropsis*: Novel integrated processes from cultivation to enzyme-assisted extraction
85 and ethanolysis of lipids. *Energy Conversion and Management*. 209 (2020) 112618.

86 [10] B.H.H. Goh, C.T. Chong, Y. Ge, H.C. Ong, J.-H. Ng, B. Tian, et al. Progress in utilisation of waste cooking
87 oil for sustainable biodiesel and biojet fuel production. *Energy Conversion and Management*. 223 (2020)
88 113296.

89 [11] R.R.C. Bastos, A.P. da Luz Corrêa, P.T.S. da Luz, G.N. da Rocha Filho, J.R. Zamian, L.R.V. da Conceição.
90 Optimisation of biodiesel production using sulfonated carbon-based catalyst from an amazon agro-
91 industrial waste. *Energy Conversion and Management*. 205 (2020) 112457.

92 [12] M. Mittelbach, H. Enzelsberger. Transesterification of heated rapeseed oil for extending diesel fuel.
93 *Journal of the American Oil Chemists' Society*. 76 (1999) 545-50.

94 [13] K.S. Al-Mawali, A.I. Osman, A.a.H. Al-Muhtaseb, N. Mehta, F. Jamil, F. Mjalli, et al. Life cycle
95 assessment of biodiesel production utilising waste date seed oil and a novel magnetic catalyst: A circular
96 bioeconomy approach. *Renewable Energy*. (2021).

97 [14] G. Knothe, L.F. Razon. Biodiesel fuels. *Progress in Energy and Combustion Science*. 58 (2017) 36-59.

98 [15] G. Knothe. 1 - Introduction. *The Biodiesel Handbook (Second Edition)*. AOCS Press 2010. pp. 1-3.

99 [16] G. Knothe. 2 - History of Vegetable Oil-Based Diesel Fuels. *The Biodiesel Handbook (Second Edition)*.
100 AOCS Press 2010. pp. 5-19.

101 [17] A.I. El-Seesy, T. Xuan, Z. He, H. Hassan. Enhancement the combustion aspects of a CI engine working
102 with *Jatropha* biodiesel/decanol/propanol ternary combinations. *Energy Conversion and Management*.
103 226 (2020) 113524.

104 [18] M.S. Habib, M. Tayyab, S. Zahoor, B. Sarkar. Management of animal fat-based biodiesel supply chain
105 under the paradigm of sustainability. *Energy Conversion and Management*. 225 (2020) 113345.

106 [19] J.E. Campbell, E. Block. Land-Use and Alternative Bioenergy Pathways for Waste Biomass.
107 *Environmental Science & Technology*. 44 (2010) 8665-9.

108 [20] P. Chhabra, S. Mosbach, I.A. Karimi, M. Kraft. Practically Useful Models for Kinetics of Biodiesel
109 Production. *ACS Sustainable Chemistry & Engineering*. 7 (2019) 4983-92.

110 [21] Erdiwansyah, R. Mamat, M.S.M. Sani, K. Sudhakar, A. Kadarohman, R.E. Sardjono. An overview of
111 Higher alcohol and biodiesel as alternative fuels in engines. *Energy Reports*. 5 (2019) 467-79.

112 [22] B. Hernández, M. Martín. Optimal Integrated Plant for Production of Biodiesel from Waste. *ACS*
113 *Sustainable Chemistry & Engineering*. (2017).

114 [23] A.a.H. Al-Muhtaseb, A.I. Osman, F. Jamil, M. Al-Riyami, L. Al-Haj, A.A. Alothman, et al. Facile technique
115 towards clean fuel production by upgrading waste cooking oil in the presence of a heterogeneous catalyst.
116 *Journal of King Saud University - Science*. 32 (2020) 3410-6.

117 [24] L.J. Konwar. New biomass derived carbon catalysts for biomass valorisation. Faculty of Science and
118 Engineering. Abo Akademi University, Turku, Finland, 2016.

119 [25] H. Li, Z. Fang, R.L. Smith Jr, S. Yang. Efficient valorisation of biomass to biofuels with bifunctional solid
120 catalytic materials. *Progress in Energy and Combustion Science*. 55 (2016) 98-194.

121 [26] A.L. de Lima, C.M. Ronconi, C.J.A. Mota. Heterogeneous basic catalysts for biodiesel production.
122 *Catalysis Science & Technology*. 6 (2016) 2877-91.

123 [27] K.Y. Wong, J.-H. Ng, C.T. Chong, S.S. Lam, W.T. Chong. Biodiesel process intensification through
124 catalytic enhancement and emerging reactor designs: A critical review. *Renewable and Sustainable Energy
125 Reviews*. 116 (2019) 109399.

126 [28] A.J. Kings, R.E. Raj, L.R.M. Miriam, M.A. Visvanathan. Cultivation, extraction and optimisation of
127 biodiesel production from potential microalgae *Euglena sanguinea* using eco-friendly natural catalyst.
128 *Energy Conversion and Management*. 141 (2017) 224-35.

129 [29] G. Chen, J. Liu, J. Yao, Y. Qi, B. Yan. Biodiesel production from waste cooking oil in a magnetically
130 fluidised bed reactor using whole-cell biocatalysts. *Energy Conversion and Management*. 138 (2017) 556-
131 64.

132 [30] G. Smith. *75 Remarkable Fruits for Your Garden*. 1 ed. Gibbs Smith 2009.

133 [31] Loquat.

134 [32] N.S. Lani, N. Ngadi, N.Y. Yahya, R.A. Rahman. Synthesis, characterisation and performance of silica
135 impregnated calcium oxide as heterogeneous catalyst in biodiesel production. *Journal of Cleaner
136 Production*. 146 (2017) 116-24.

137 [33] A.a.H. Al-Muhtaseb, F. Jamil, M.T.Z. Myint, M. Baawain, M. Al-Abri, T.N.B. Dung, et al. Cleaner fuel
138 production from waste Phoenix dactylifera L. kernel oil in the presence of a bimetallic catalyst:
139 Optimisation and kinetics study. *Energy Conversion and Management*. 146 (2017) 195-204.

140 [34] H.H. Mardhiah, H.C. Ong, H.H. Masjuki, S. Lim, Y.L. Pang. Investigation of carbon-based solid acid
141 catalyst from *Jatropha curcas* biomass in biodiesel production. *Energy Conversion and Management*. 144
142 (2017) 10-7.

143 [35] F.H. Alhassan, U. Rashid, Y.H. Taufiq-Yap. Synthesis of waste cooking oil-based biodiesel via effectual
144 recyclable bi-functional Fe₂O₃MnOSO₄2-/ZrO₂ nanoparticle solid catalyst. *Fuel*. 142 (2015) 38-45.

145 [36] M. Farooq, A. Ramli, D. Subbarao. Biodiesel production from waste cooking oil using bifunctional
146 heterogeneous solid catalysts. *Journal of Cleaner Production*. 59 (2013) 131-40.

147 [37] F. Jamil, A.a. Al-Muhtaseb, M.T.Z. Myint, M. Al-Hinai, L. Al-Haj, M. Baawain, et al. Biodiesel production
148 by valorising waste Phoenix dactylifera L. Kernel oil in the presence of synthesised heterogeneous metallic
149 oxide catalyst (Mn@MgO-ZrO₂). *Energy Conversion and Management*. 155 (2018) 128-37.

150 [38] A. Chamkalani, S. Zendejboudi, N. Rezaei, K. Hawboldt. A critical review on life cycle analysis of algae
151 biodiesel: current challenges and future prospects. *Renewable and Sustainable Energy Reviews*. 134
152 (2020) 110143.

153 [39] S. Zendejboudi, I. Chatzis, A.A. Mohsenipour, A. Elkamel. Dimensional Analysis and Scale-up of
154 Immiscible Two-Phase Flow Displacement in Fractured Porous Media under Controlled Gravity Drainage.
155 *Energy & Fuels*. 25 (2011) 1731-50.

156 [40] A.I. Osman, J. Meudal, F. Laffir, J. Thompson, D. Rooney. Enhanced catalytic activity of Ni on η-Al₂O₃
157 and ZSM-5 on addition of ceria zirconia for the partial oxidation of methane. *Applied Catalysis B:
158 Environmental*. 212 (2017) 68-79.

159 [41] S. Caschili, F. Delogu, A. Concas, M. Pisu, G. Cao. Mechanically induced self-propagating reactions:
160 Analysis of reactive substrates and degradation of aromatic sulfonic pollutants. *Chemosphere*. 63 (2006)
161 987-95.

162 [42] A. Imtiaz, M.A. Farrukh, M. Khaleeq-ur-rahman, R. Adnan. Micelle-Assisted Synthesis of
163 Al₂O₃-CaO Nanocatalyst: Optical Properties and Their Applications in
164 Photodegradation of 2,4,6-Trinitrophenol. *The Scientific World Journal*. 2013 (2013) 641420.

- 165 [43] X. Yu, Z. Wen, H. Li, S.-T. Tu, J. Yan. Transesterification of Pistacia chinensis oil for biodiesel catalysed
166 by CaO–CeO₂ mixed oxides. *Fuel*. 90 (2011) 1868-74.
- 167 [44] W.N.N. Wan Omar, N.A.S. Amin. Biodiesel production from waste cooking oil over alkaline modified
168 zirconia catalyst. *Fuel Processing Technology*. 92 (2011) 2397-405.
- 169 [45] A.N. Narayanappa, P.V. Kamath. Interaction of Pristine Hydrocalumite-Like Layered Double
170 Hydroxides with Carbon Dioxide. *ACS Omega*. 4 (2019) 3198-204.
- 171 [46] G. Barjoveanu, O.-A. Pătrăuțanu, C. Teodosiu, I. Volf. Life cycle assessment of polyphenols extraction
172 processes from waste biomass. *Scientific Reports*. 10 (2020) 13632.
- 173 [47] A. Fridrihsone, F. Romagnoli, U. Cabulis. Environmental Life Cycle Assessment of Rapeseed and
174 Rapeseed Oil Produced in Northern Europe: A Latvian Case Study. *Sustainability*. 12 (2020) 5699.
- 175 [48] W. Thitsartarn, S. Kawi. An active and stable CaO–CeO₂ catalyst for transesterification of oil to
176 biodiesel. *Green Chemistry*. 13 (2011) 3423-30.
- 177 [49] Instrument mixer - https://shop.teknomatik.co.uk/en_US/p/IBC-pneumatic-mixer-MKP-5000-Ex/43 ,
178 accessed on 10-2-2021 5pm.
- 179 [50] Autoclave electricity consumption. Available at: <https://labstac.com/Horizontal-Autoclave/p/AH115>,
180 accessed 10-2-2021 3 pm.
- 181 [51] Oven electricity requirement. Available at:
182 <http://www.keison.co.uk/products/carbolite/LaboratoryIndustrialOvensandFurnaces.pdf> , accessed 10-
183 2-2021 4pm.
- 184 [52] M.H. Mohammadi Ashnani, A. Johari, H. Hashim, E. Hasani. Life Cycle Assessment of Palm Oil Biodiesel
185 Production in Malaysia. *Applied Mechanics and Materials*. 465-466 (2014) 1080-6.
- 186 [53] Z.L. Chung, Y.H. Tan, Y.S. Chan, J. Kandedo, N.M. Mubarak, M. Ghasemi, et al. Life cycle assessment
187 of waste cooking oil for biodiesel production using waste chicken eggshell derived CaO as catalyst via
188 transesterification. *Biocatalysis and Agricultural Biotechnology*. 21 (2019) 101317.
- 189 [54] S. Photaworn, C. Tongurai, S. Kungsanunt. Process development of two-step esterification plus
190 catalyst solution recycling on waste vegetable oil possessing high free fatty acid. *Chemical Engineering
191 and Processing: Process Intensification*. 118 (2017) 1-8.
- 192 [55] L. Lardon, A. Hélias, B. Sialve, J.-P. Steyer, O. Bernard. Life-Cycle Assessment of Biodiesel Production
193 from Microalgae. *Environmental Science & Technology*. 43 (2009) 6475-81.
- 194 [56] E.G. Hertwich, S.F. Mateles, W.S. Pease, T.E. McKone. Human toxicity potentials for life-cycle
195 assessment and toxics release inventory risk screening. *Environmental Toxicology and Chemistry*. 20
196 (2001) 928-39.
- 197 [57] P.P. Kalbar, M. Birkved, S.E. Nygaard, M. Hauschild. Weighting and Aggregation in Life Cycle
198 Assessment: Do Present Aggregated Single Scores Provide Correct Decision Support? *Journal of Industrial
199 Ecology*. 21 (2017) 1591-600.
- 200 [58] A.F. Clarens, E.P. Resurreccion, M.A. White, L.M. Colosi. Environmental Life Cycle Comparison of Algae
201 to Other Bioenergy Feedstocks. *Environmental Science & Technology*. 44 (2010) 1813-9.

202